

Estimating Treatment Effects under Recommender Interference: A Structured Neural Networks Approach

Ruohan Zhan
rhzhan@ust.hk
The Hong Kong University of
Science and Technology

Shichao Han
shichaohan@tencent.com
Tencent Inc.

Yuchen Hu
yuchenhu@stanford.edu
Stanford University

Zhenling Jiang*
zhenling@wharton.upenn.edu
University of Pennsylvania

Abstract

Recommender systems are essential for content-sharing platforms by curating personalized content. To evaluate updates of recommender systems targeting content creators, platforms frequently engage in creator-side randomized experiments to estimate treatment effect, defined as the difference in outcomes when a new (vs. the status quo) algorithm is deployed on the platform. We show that the standard difference-in-means estimator can lead to a biased treatment effect estimate. This bias arises because of recommender interference, which occurs when treated and control creators compete for exposure through the recommender system. We propose a “recommender choice model” that captures how an item is chosen among a pool comprised of both treated and control content items. By combining a structural choice model with neural networks, the framework directly models the interference pathway in a microfounded way while accounting for rich viewer-content heterogeneity. Using the model, we construct a double/debiased estimator of the treatment effect that is consistent and asymptotically normal. We demonstrate its empirical performance with a field experiment on Weixin short-video platform: besides the standard creator-side experiment, we carry out a costly blocked double-sided randomization design to obtain a benchmark estimate without interference bias. We show that the proposed estimator significantly reduces the bias in treatment effect estimates compared to the standard difference-in-means estimator.

Key words: Recommender Interference; Average Treatment Effect; Online Content Platforms; Creator-side Randomization; Choice Model; Neural Networks; Double/Debiased Estimation and Inference

We are grateful to Susan Athey, Tat Chan, Wanning Chen, Yue Fang, Bryan Graham, Ganesh Iyer, Ramesh Johari, Hannah Li, Ilan Lobel, Xiaojie Mao, Tu Ni, Nian Si, Zikun Ye, Dennis Zhang, Jinglong Zhao, conference participants at CODE@MIT 2023 and ACIC 2024, and seminar attendees at University of Washington, National University of Singapore, Tsinghua University, The Chinese University of Hong Kong (Shenzhen) for their helpful comments. The short version of this paper has appeared in the ACM Conference on Economics and Computation (EC’24), and we are especially thankful to the anonymous reviewers for their constructive feedback. We are grateful to the WeChat Experimentation Team at Tencent for their generous support, particularly Darwin Yong Wang, who has helped shape and advance this work’s applications in the online platform domain.

*Corresponding author.

1. Introduction

Recommender systems (RecSys) are at the heart of online content platforms by curating viewer-specific content selections based on data sources such as profiles and past interactions. Indeed, recommendation plays a significant role in driving content consumption for viewers (Kiros 2022). This is particularly the case for short-video platforms such as TikTok, where viewers are directly presented with a stream of videos in the For-You feed determined by the recommendation algorithm.

Recognizing the importance of RecSys, platforms regularly develop and assess new algorithms. In this paper, we focus on the ones aimed at improving the experience of content creators. Platforms rely on creators to generate a diverse and vibrant content pool (Mehrotra et al. 2018, Rosen 1981), which ensures viewer satisfaction and platform success in the long term. Platforms engage in multiple strategies to incentivize creators. As an example, recommendation algorithms may boost the visibility of content by new creators to mitigate the “cold-start” problem. They can also allocate more traffic to creators with higher-quality content or those who pay for more exposure.

To evaluate the performance of these creator-focused algorithm updates, platforms typically rely on experiments with “creator-side randomization”. This involves randomly assigning a group of creators in the treatment group, served by the new algorithm, and the others in the control group, served by the status quo algorithm, following standard A/B testing protocols. The treatment effect is typically measured using the Difference-in-Means (DIM) estimator, which compares the average outcomes between the treatment vs. control groups, such as how many likes creators receive.

We show that the standard DIM estimator can lead to biased treatment effect estimates. This is because the outcomes of creators are influenced not only by their own treatment status but also by the statuses of their peers, violating the Stable Unit Treatment Value Assumption (SUTVA) (Imbens 2004). Such peer effects are due to that treated and control creators compete for exposure through the recommendation algorithm. This competition in the content recommendation stage causes outcomes in one group to depend on creators in another group, a phenomenon known as “interference” or “spill-over effects” (Johari et al. 2022, Bajari et al. 2021). As an example, an algorithm that boosts exposure for new creators may work well in a small-scale treatment group when considered along with other new creators without the boost in the control group, but fails to generalize upon full-scale implementation when all new creators receive the boost. Indeed, in our empirical context (in Weixin, China’s analog of WeChat), there is often a large discrepancy in an algorithm’s performance in small-scale A/B testing vs. full-scale implementation.¹

¹ Such discrepancies can arise from multiple factors, including interference, nonstationarity, etc. This is a key highlight of our empirical study, where we concurrently compare algorithm performances in both settings. With that, we can attribute the primary source of the discrepancy to interference; see more details in Section 5.

When evaluating recommendation algorithms, the true outcome of interest is the “average treatment effect” (ATE), defined as the difference between expected outcomes when a new algorithm is fully scaled on the platform (referred to as “global treatment”), vs. when the status quo is deployed (referred to as “global control”). Importantly, the DIM estimator can either overestimate or underestimate the ATE, sometimes even with the reversed sign (Dhaouadi et al. 2023). Relying on the DIM estimator to determine which algorithm to scale up poses significant challenges for data-driven decision-making.

In this paper, we propose an approach to directly estimate the ATE when platforms conduct experiments with creator-side randomization. We do so by modeling how recommendation algorithms choose a content item to expose to viewers from a content pool comprised of both treated and control content items. This “recommender choice model” captures the interference pathway: outcomes of treated content items are affected by the control group because they can be in the same pool competing for exposure. The choice model can rationalize and predict that outcomes can differ in small-scale A/B testing, when treated content items compete with other control content items, and in full-scale implementation, when all content items are treated.

To implement this approach, we estimate the recommender choice model using data from creator-side experiments. The estimated model describes which content item gets exposed to the viewer from a pool of content and how their treatment status affects the exposure process. The ATE estimate is the difference in outcomes between two counterfactual scenarios: when all content items are treated and when all content items are in control. The model leverages an insight that different recommendation algorithms have different ways of calculating the “score” of an item for each viewer, which essentially drives the recommendation. For example, an algorithm focused on cold-start problems will assign a higher score for new creators. We use separate flexible neural nets to capture the potentially complex mapping from viewer-content pairs to their scores under treatment and control conditions.

Methodologically, the proposed approach combines a structural choice model with flexible neural nets. The structural choice model framework is important since it facilitates counterfactual evaluations under alternative treatment assignments (e.g., all treated or all control). Such evaluations can be at the population level (such as the ATE) or at the sub-population level (such as the conditional average treatment effect or CATE). This is achieved since our choice model captures the key interference pathway by directly modeling how content items compete for exposure in a micro-founded way. The neural nets in the choice model are important to capture the nuances in how *personalized* recommendation algorithms score content items by accounting for rich viewer-content heterogeneity. This would be very hard to do using a parametric model, unlike in settings with only structured attributes such as price and brand. Building upon semiparametric literature

Table 1 Experimental design of verification experiments

| | Creator 1 | Creator 2 | Creator 3 | Creator 4 | Creator 5 | Creator 6 |
|----------|----------------|----------------|----------------|----------------|----------------|----------------|
| Viewer 1 | <i>C</i> | <i>C</i> | <i>Blocked</i> | <i>Blocked</i> | <i>Blocked</i> | <i>Blocked</i> |
| Viewer 2 | <i>C</i> | <i>C</i> | <i>Blocked</i> | <i>Blocked</i> | <i>Blocked</i> | <i>Blocked</i> |
| Viewer 3 | <i>Blocked</i> | <i>Blocked</i> | <i>T</i> | <i>T</i> | <i>Blocked</i> | <i>Blocked</i> |
| Viewer 4 | <i>Blocked</i> | <i>Blocked</i> | <i>T</i> | <i>T</i> | <i>Blocked</i> | <i>Blocked</i> |
| Viewer 5 | <i>Blocked</i> | <i>Blocked</i> | <i>Blocked</i> | <i>Blocked</i> | <i>C</i> | <i>T</i> |
| Viewer 6 | <i>Blocked</i> | <i>Blocked</i> | <i>Blocked</i> | <i>Blocked</i> | <i>C</i> | <i>T</i> |

Note: The market is segmented into three distinct worlds, with viewers in each world receiving recommendations exclusively for content produced by creators within their respective world. The first world (with viewers and creators 1 and 2) uses the control algorithm, and the second world (with viewers and creators 3 and 4) applies the treatment algorithm — the design involving these two worlds is known as blocked double-sided randomization. In the third world (with viewers and creators 5 and 6) a standard creator-side experiment is conducted, assigning creators randomly to treatment or control algorithms. To reduce market size impact, the viewer count across all three worlds is equalized.

(Chernozhukov et al. 2018, 2019, Farrell et al. 2020), we construct an estimator of ATE that is consistent and asymptotically normal. We substantiate our theoretical guarantees with simulations, showing that the proposed approach gives valid estimation and inference results.

We demonstrate the empirical performance of the proposed approach using experimental data from the Weixin short-video platform. Unlike simulated scenarios with a known ground truth, real-world data lack a direct benchmark. To approximate the ATE without interference bias, we carry out a blocked double-sided randomization design (Bajari et al. 2021, Su et al. 2024) in addition to the standard creator-side randomized experiment. As shown in Table 1, we divide the viewers and creators on the platform into three distinct worlds. The first world implements the control algorithm, and the second world implements the treatment algorithm; observing these two alternative worlds at the same time allows us to approximate ATE by the difference in outcomes across the two worlds. The third world implements the standard creator-side experiment where creators are randomly assigned to treatment and control conditions. Using data from the creator-side experiment, we compute the treatment effect with both standard DIM and our debiased estimators. Compared to the approximated ATE from the blocked double-sided experiment, we show that our method significantly reduces the bias in treatment effect estimates compared to the standard DIM estimator.

The blocked double-sided randomization mitigates bias by blocking viewers from accessing content items from another world, so that the control and treated content items are no longer competing with each other. Despite its effectiveness, implementing such a strategy to estimate treatment effects is very costly. It requires significant engineering effort to modify the experimental infrastructure, and the market size is effectively cut in half for both viewers and creators. Moreover, the

population under a blocked double-sided design cannot be reused for other orthogonal experiments, which is not the case for single-side randomization designs.

Another commonly applied experimental design that we have not discussed yet involves randomly assigning viewers to treatment vs. control recommendation algorithms. Given our focus on treatment targeting at creators, assessed through creator-centric outcomes such as the increase in likes, randomizing on the creator side serves as a more natural design over viewer-side randomization. Additionally, viewer-side randomization design introduces its own source of interference bias. This is because content items are served to both treatment and control viewers, as a result, the outcomes from one condition will affect the other condition. For example, new creators will receive more exposure and likes from viewers assigned to the treatment “cold-start” algorithm, but because of the higher interaction received, these creators will also receive more exposure and likes from viewers in the control group without the boost. Broadly speaking, reactions from both treatment and control viewers contribute to the item embeddings simultaneously, causing the so-called “symbiosis bias” as documented in [Holtz et al. \(2023a\)](#), [Si \(2023\)](#).

This paper contributes to a growing literature that documents and proposes solutions to mitigate interference bias in two-sided marketplaces. We identify interference during the recommendation stage when treated and control content items compete for exposure, and show that the standard DIM estimator leads to a biased estimate of ATE. This exposure interference pathway is distinct from other sources of interference identified in online platforms, such as ranking and viewer-Markovian interference ([Goli et al. 2023](#), [Farias et al. 2023](#)). To model the interference pathway, we propose a novel framework that combines a structural choice model with neural nets, which allows us to directly estimate the ATE. This approach is distinct from a stream of work that aims to develop novel experimental designs to minimize interference during the experiment ([Holtz and Aral 2020](#), [Holtz et al. 2023b](#), [Ugander et al. 2013](#), [Johari et al. 2022](#), [Bajari et al. 2021](#)). For online content platforms, such an approach is impractical because of the interconnected networks. For example, one needs to design randomization in a way that treatment and control groups never appear in the same pool of consideration to avoid them competing for exposure, which is hard to accomplish in our setting. We validate the proposed approach using experimental data on a leading short-video platform. We are fortunate to have carried out a blocked double-sided randomization design as validation for our proposed approach, which is one of the initial attempts in the literature to empirically approximate the ground truth ATE under interference.

1.1. Related Literature

There has been a growing research focus on studying randomized experiments with cross-unit interference. This issue refers to scenarios where an individual’s outcome is affected by others’

treatments, violating the Stable Unit Treatment Value Assumption (SUTVA) in classical causal inference (Imbens and Rubin 2015, Imbens 2004). This interference effect can be local in the neighborhood, where treatments only spill over among individuals connected in a graph (Ugander et al. 2013, Aronow and Samii 2017, Leung 2020, Li and Wager 2020), clustered within groups or communities, where individuals outside of a cluster have no peer effect on the individuals inside a cluster (Hudgens and Halloran 2008, Tchetgen and VanderWeele 2012, Johari et al. 2022), or global via a structured equilibrium effect, where interference is mediated through a global system parameter in large-scale stochastic systems (Wager and Xu 2021, Munro et al. 2021, Li et al. 2023). Each of these interference forms presents unique challenges and may appear in online marketplaces.

Interference complicates the estimation of treatment effects in online marketplaces, leading to biased results under standard A/B testing framework across various contexts (Sävje et al. 2021, Hu et al. 2021, Farias et al. 2022, Johari et al. 2022, Dhaouadi et al. 2023, Zhu et al. 2024). To address such bias arising from interference, the literature has pursued two primary research directions. The first line proposes innovative experimental designs to mitigate interference. Popular methods include clustered randomization design, which groups units to minimize interference between clusters and then randomizes treatment at the cluster level (Holtz and Aral 2020, Holtz et al. 2023b, Ugander et al. 2013, Hudgens and Halloran 2008), and switchback design, which assigns target intervention randomly at the market level across different time periods (Bojinov et al. 2023, Hu and Wager 2022, Ni et al. 2023, Xiong et al. 2023). Both however are not directly applicable to our settings since we do not have an explicit graph for clustering in the former case, and the content markets are too interconnected to isolate a clean experimental population for the latter.

We note two types of experimental designs that are particularly relevant to our settings. The first one is two-sided or double-sided randomization, where viewers and creators are jointly clustered into blocks and randomized into treatment and control groups together. When cross-treatment interactions between the two sides are allowed, results are mainly established for homogeneous units—an assumption that is unrealistic in the personalized recommendation context due to the intrinsic viewer-content heterogeneity (Johari et al. 2022, Bajari et al. 2021, Munro et al. 2023). Conversely, when cross-treatment interactions are explicitly disallowed, as in the blocked double-sided randomization we adopt in our empirical context, the approach is too expensive for large-scale implementation (Ye et al. 2023a, Su et al. 2024). The second approach involves generating counterfactual interleaving ranking during the content recommendation phase, such that items in the treatment group are ranked the same during the A/B testing as in the global treatment scenarios Wang and Ba (2023), Ha-Thuc et al. (2020). However, implementing this design within the current recommendation infrastructure requires significant engineering efforts; it may also increase latency in online serving, potentially degrading the viewer experience.

The second line to address interference adheres to the existing A/B testing infrastructure but proposes new estimators beyond the standard DIM, to which our work contributes. This requires domain-specific analysis of interference types. For example, [Goli et al.](#) address bias in ranking experiments by using historical A/B test data to construct a deep learning model for ATE estimation, focusing on content items with positions close to those under the true counterfactual equilibrium. [Bright et al.](#) model the interference in the generalized matching setting, where the platform solves the matching via a linear programming algorithm, leveraging which they propose a shadow-price based estimator to mitigate interference bias. [Farias et al.](#) introduce a model that incorporates a Markovian structure to model viewer behavior, addressing interference arising from viewer-side state transition during continuous platform engagement. This paper focuses on interference during platform algorithm operations phase, where treated and control creators compete to get recommended by the system. Unlike previous studies, we also develop confidence intervals beyond point estimates of ATE, facilitating hypothesis testing. This addition is crucial for tech companies that need type-I error control for their extensive daily A/B testing experiments.

Our results are built upon recent advances in causal machine learning and semiparametric inference ([Newey 1994](#), [Chernozhukov et al. 2018](#), [Farrell et al. 2020](#), [Chernozhukov et al. 2019](#)). We particularly note the innovative development of doubly robust estimators by [Farrell et al.](#) for semiparametric modeling, wherein the outcome model is parametric in treatment but non-parametric in the observed context; this method is the key foundation that our paper builds upon. The application of this method in online platforms has been pioneered by [Ye et al.](#) to infer the causal effects of combinatorial experiments. This paper adapts it to analyzing interference in the recommendation phase, where we combine a parametric structural choice model ([Train 2009](#)), representing recommender behavior, with non-parametric machine learning models to address individual-level heterogeneity common in platform data. We believe this integration of structural modeling with machine learning shows a promising direction in addressing platform-related challenges.

Finally, our paper also connects to the long-standing literature on recommender systems that address item exposure bias ([Liang et al. 2016](#), [Schnabel et al. 2016](#), [Ma and Chen 2019](#)). Specifically, items displayed by the recommender are more likely to receive favorable responses from viewers, whereas responses for items not displayed are missing, not at random. This selection bias, if uncorrected, is reinforced when biased samples are used for the subsequent training rounds of recommendation algorithms, which can prevent these algorithms from accurately learning underlying viewer preferences. This phenomenon, known as the “feedback loop” in recommender systems, has received increasing attention from both academia and industry ([Sinha et al. 2016](#), [Chaney et al. 2018](#), [Sun et al. 2019](#), [D’Amour et al. 2020](#), [Mansoury et al. 2020](#)).

2. Interference in Recommender System Experiments

This section frames our study within the context of an industry-standard recommender system. We start with an overview of creator-side recommender experiments and introduce notations to formulate the treatment effect estimation problem. We then discuss how interference arises in the recommendation process. We conclude this section by showing the bias of the commonly applied difference-in-means estimator in our setting.

2.1. Creator-side Recommender Experiments

Recommender systems (RecSys) are designed to serve personalized content for viewers from a large corpus comprised of potentially billions of content items. The overall goal is to score the content items according to their likelihood of engaging the user (e.g., expected viewing time and interactions such as likes and shares). The industry-standard recommendation process is a long pipeline consisting of three main stages: retrieval, ranking, and re-ranking, where the pool of consideration gets decreasingly smaller. In the retrieval stage, the system starts by selecting content items from a vast pool using efficient and scalable algorithms. In the ranking stage, these content items are prioritized with the predicted relevance to the user. Finally, the re-ranking stage fine-tunes the recommendations and often considers other factors such as cold-start or advertising. In our context, the recommender system selects one item in response to each viewer query (e.g., swiping for the next video) instead of presenting an ordered list.²

Platforms frequently update their recommender system, which involves anywhere from adjusting algorithm hyper-parameters to implementing a new algorithm. Platforms use experiments to compare against the current benchmark and decide whether to adopt the update. We define several terminologies. *Treatment* denotes an updated recommender system, while *control* is the current status-quo. We use *consideration set* to denote the pool of content for consideration by the recommender system. The treatment vs. control algorithms score content items differently and therefore will lead to different *exposure probabilities* of content items given a consideration set.

The focus of this paper is on “creator-side” algorithm updates that happen at the re-ranking stage. Because of the focus on creators, platforms frequently rely on creator-side experiments where creators (as opposed to users) are randomized to use the treatment vs. control algorithms for scoring.³ Because of the focus on the re-ranking stage, the consideration set tends not to be large. However, it can include items from both treatment and control groups that are scored with the

² Our framework can be extended to multi-item recommendations with an alternative choice model that selects multiple content items for each viewer query.

³ We use creator and content interchangeably in this paper. In practice, content items inherit treatment status from their creators, and creators assess their experience based on the outcomes of their content items.

corresponding algorithms. One item from the consideration set is exposed to the viewer, and we measure its outcomes from viewer-content interactions, such as view time or likes.⁴

We now introduce notations to describe the data structure from a creator-side experiment. Each observation i is from a viewer query where one item is exposed to the viewer. We observe a tuple $(V_i, \vec{C}_i, \vec{W}_i, k_i^*, Y_i)$, where V_i denotes the viewer and $\vec{C}_i = \{C_{i,1}, \dots, C_{i,K}\}$ denotes the consideration set of K content items.⁵ Content items are randomized into treatment with probability q , or control with probability $1 - q$, via i.i.d. Bernoulli trials.⁶ $\vec{W}_i = \{W_{i,1}, \dots, W_{i,K}\}$ indicates the treatment status for each item in the set, with $W_{i,k} = 1$ for treated and $W_{i,k} = 0$ for control. Content k_i^* is exposed to the viewer, and the outcome variable Y_i measures the viewer’s response to the recommended content.

It is useful to clarify what components are affected by the experimental interventions in our framework. The consideration set \vec{C}_i is not affected because we focus on experiments that occur after the retrieval system forms the consideration set. What item gets exposed k_i^* is affected by the experiments. In fact, modeling item exposure conditional on treatment assignment is the focus of the recommender choice model that we introduce in the next section. The viewer’s response Y_i is affected by the experimental interventions only through which item is exposed. Conditional on exposure, the response Y_i only depends on the viewer V_i and content C_{i,k^*} pair and not the content’s treatment status. Since we do not consider the temporal interference of viewers, we can take each viewer query as an i.i.d. sample.

2.2. Formulate ATE using Policy Value

We introduce notations for treatment effect estimation under creator-side experiments following the potential outcome framework (Imbens and Rubin 2015). Let $w_c \in \{0, 1\}$ denote the treatment status for content item c .⁷ Let \mathbf{w}_{-c} collect the treatment statuses of all content items except for c . Let $y(v, c; w_c, \mathbf{w}_{-c})$ denote content c ’s potential outcome from viewer v with treatment assignment $\mathbf{w} = [w_c, \mathbf{w}_{-c}]$. By convention, we let the potential outcome $y(v, c; w_c, \mathbf{w}_{-c})$ be zero if content c is not recommended to viewer v .

The outcome of interest for content c under treatment assignment (w_c, \mathbf{w}_{-c}) is the expected value over the distribution of viewer v :

$$r(c; w_c, \mathbf{w}_{-c}) := \mathbb{E}_v [y(v, c; w_c, \mathbf{w}_{-c})]. \quad (1)$$

⁴ These viewer-content outcomes serve as the building blocks that affect creator-level outcomes such as the frequency of content creation, which we abstract away from in this paper.

⁵ Extension to accommodating various sizes of consideration sets is straightforward, and here we focus on cases with the same set size for notation convenience.

⁶ Although randomization typically happens at the creator level in practice, with content items inheriting their treatment status, our setting simplifies to content-level randomization for notation convenience.

⁷ Our discussion focuses on a binary treatment for notational brevity. The framework can be easily extended to multiple treatments (details in Appendix E).

Let policy π specify the treatment assignment rule. The policy value $Q(\pi)$ measures the overall outcome across the content set \mathcal{C} under treatment assignment policy π (Johari et al. 2022, Goli et al. 2023):

$$Q(\pi) := \mathbb{E}_{\mathbf{w}_{-c} \sim \pi} \left[\sum_{c \in \mathcal{C}} r(c; w_c, \mathbf{w}_{-c}) \right]. \quad (2)$$

Let π_1 denote the global treatment policy where all content items use the treatment algorithm ($w_c, \mathbf{w}_{-c} = \mathbf{1}$) and π_0 denote the global control policy where all items use the control algorithm ($w_c, \mathbf{w}_{-c} = \mathbf{0}$). The outcome of interest, ATE, is defined as the difference between the policy values of global treatment versus global control.

$$\tau := Q(\pi_1) - Q(\pi_0) = \sum_{c \in \mathcal{C}} \{r(c; \mathbf{1}) - r(c; \mathbf{0})\}. \quad (3)$$

2.3. Recommender Interference and Bias of DIM Estimator

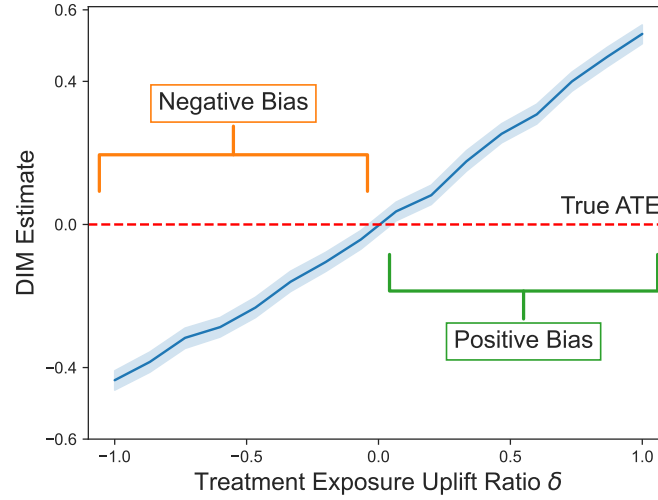
Interference arises in the recommendation process because content items are “competing for exposure” from the consideration set. Since both treated and control items can appear in the same consideration set, the scoring from the treatment algorithm can influence the exposure probabilities of control content items, and vice versa. As a result, the outcomes of content items depend not only on their own treatment status but also on the treatment status of the other content items, violating the SUTVA assumption.

Using notations introduced in Section 2.2, recommender interference arises because the potential outcome for content c , $y(v, c; w_c, \mathbf{w}_{-c})$, depends not only on its own treatment status w_c but also on the treatment status of all other content \mathbf{w}_{-c} . Generally, with $\mathbf{w}_{-c}^{(a)} \neq \mathbf{w}_{-c}^{(b)}$, the potential outcomes also differ: $y(v, c; w_c, \mathbf{w}_{-c}^{(a)}) \neq y(v, c; w_c, \mathbf{w}_{-c}^{(b)})$. As discussed in Section 2.1, the outcomes differ with treatment assignments because they affect the exposure probability of the focal item c .

Because of the recommender interference, the difference-in-means estimator (DIM) leads to a biased estimate of the treatment effect. Using data from creator-side experiments as described in Section 2.1, the commonly adopted DIM estimator takes the form (Bright et al. 2022, Goli et al. 2023, Johari et al. 2022):

$$\hat{\tau}_n^{DIM} := \frac{\sum_{i=1}^n \mathbf{1}\{W_{i,k_i^*} = 1\} Y_i}{nq} - \frac{\sum_{i=1}^n \mathbf{1}\{W_{i,k_i^*} = 0\} Y_i}{n(1-q)}, \quad (4)$$

where n is the number of observations. The treatment effect estimated using DIM, $\hat{\tau}_n^{DIM}$, is the difference in outcomes between items assigned to treatment ($W_{i,k_i^*} = 1$) relative to those in control ($W_{i,k_i^*} = 0$). Since the DIM estimator does not consider the “competition” that happens between treated and control items, the estimator does not measure the ground truth ATE of interest, which is the difference in outcomes under global treatment compared to global control (as in Eq. 3).

Figure 1 Illustrative Example of the Bias of the DIM Estimator

We start by illustrating the bias of the DIM estimator using a simple example. Consider an extreme case where the outcome is the same across all viewer-content pairs, such as the view metric that equals 1 for the exposed content and 0 otherwise. In such a case, the true ATE is zero because each viewer query always exposes one item no matter what recommender algorithm is applied. Suppose the treatment algorithm adds an uplift δ to the scoring relative to the control algorithm. When $\delta > 0$, the exposure probability of items in treatment is larger than that in control (i.e., a boosting effect). When $\delta < 0$, the reverse happens (i.e., a suppression effect).

Figure 1 illustrates the bias of the DIM estimator using this extreme example where the true ATE is zero (the red dotted line). We simulate data using different values of δ and compute the DIM estimates (detailed simulation settings are described in Section 4.3). The blue line shows the DIM estimates across different uplift δ averaged over 1000 simulations with the shaded area indicating 95% confidence intervals. The bias of the DIM estimator can be either positive or negative, depending on how competition influences the items' exposure probabilities. When $\delta > 0$, the estimate using DIM is positive because items in treatment are exposed more than those in control, leading to a positive bias compared to the true ATE at zero. When $\delta < 0$, items in treatment are less likely to be exposed and the DIM estimate has a negative bias.

This simple example illustrates that the DIM estimator (Eq. 4) does not measure the ATE and the bias can be either positive or negative. We characterize the asymptotic behavior of the DIM estimator as the sample size n grows, and show that it converges to a quantity different than the ATE (Eq. 3). To do so, we introduce an assumption that constrains the number of consideration sets each item appears in, similar to those in prior literature (Viviano 2019, Sävje et al. 2021).

ASSUMPTION 1 (Bounded item appearance). *Let n be the sample size. Each item appears in at most a_n consideration sets, with $a_n = o(n^{1/4})$.*

This assumption ensures that the number of randomization units (i.e., content items) scales with the sample size. In practical terms, this assumption is often satisfied in real-world applications with creator-side experiments. These experiments typically target items produced by small creators or for advertising purposes, where the number of consideration sets they appear in is relatively small compared to the overall sample size.

PROPOSITION 1 (Convergence of the difference-in-means estimator). *Suppose Assumption 1 holds. Under the creator-side randomization with treated probability $q \in (0, 1)$, the difference-in-means estimator $\hat{\tau}_n^{DIM}$ converges in probability to a quantity $\tau^{B(q)}$,*

$$\hat{\tau}_n^{DIM} \xrightarrow{p} \tau^{B(q)} \quad \text{where} \quad \tau^{B(q)} := \mathbb{E} \left[\sum_{c \in \mathcal{C}} \{r(c; w_c = 1, \mathbf{w}_{-c} \sim \mathcal{B}(q)) - r(c; w_c = 0, \mathbf{w}_{-c} \sim \mathcal{B}(q))\} \right], \quad (5)$$

with $\mathbf{w}_{-c} \sim \mathcal{B}(q)$ denoting that the treatment status of all content items except for c is sampled from a Bernoulli distribution with a treatment probability of q .

Detailed proof is given in the appendix. The quantity $\tau^{B(q)}$ is often referred to as the direct effect of the treatment under creator-side randomization (Sävje et al. 2021, Hu et al. 2021). The difference between $\tau^{B(q)}$ and the ATE τ is “interference bias”. Similar results have been established in two-sided matching platforms such as ride-sharing (Bright et al. 2022).

3. Modeling Interference

In this section, we introduce a recommender choice model to explicitly account for interference during the recommendation phase. This semi-parametric model incorporates neural networks in the choice model in order to flexibly capture personalized recommendations based on diverse viewer preferences and content characteristics. We use counterfactual analysis for treatment effect estimation. We conclude this section by discussing the scope of the proposed approach: what types of interference it does and does not capture.

3.1. Recommender Choice Model

Upon a viewer query, the goal of the recommender system is to choose the most suitable content item for viewer V_i from the consideration set \vec{C}_i . Inspired by the concept of *model distillation* (Hinton et al. 2015), we represent the complex recommender system using a choice model, which describes how the recommender system “chooses” from a list of items in the consideration set.

The score or “utility” of content $C_{i,k}$ for viewer V_i takes the form:

$$S_{i,k} = s_0(V_i, C_{i,k}) + W_{i,k} \cdot s_1(V_i, C_{i,k}) + \epsilon_{i,k}. \quad (6)$$

The baseline score function $s_0(\cdot, \cdot)$ approximates the control algorithm’s evaluation of content given viewer V_i and content $C_{i,k}$. For items in the treatment group ($W_{i,k} = 1$), $s_1(\cdot, \cdot)$ captures the score uplift from the treatment algorithm’s evaluation of content $C_{i,k}$ for viewer V_i .⁸ We parameterize the score functions $s_0(\cdot, \cdot)$ and $s_1(\cdot, \cdot)$ as neural networks. Neural nets can flexibly capture the relationship between recommender scoring and the viewer-content pairs, which effectively approximate the personalized recommendations for different viewers (Covington et al. 2016).

The error term $\epsilon_{i,k}$ represents the part of content evaluation that score functions s_0 and s_1 do not capture. It accounts for the inherent randomness in recommender systems as well as the approximation errors of these neural nets in representing the actual recommender pipeline.⁹ Randomness in the recommendations can arise from concurrent orthogonal experiments, a common practice among tech companies (Ivaniuk and Duan 2020), as well as system-wide uncertainties, such as viewers being assigned less sophisticated algorithms to reduce latency during peak hours (Taylor and Wexler 2003). We assume that the error term $\epsilon_{i,k}$ follows an i.i.d. Type 1 Extreme Value distribution, and the item with the highest score or “utility” in the consideration set will be exposed to viewer V_i .

With these assumptions, we can write the choice probability using the multinomial logit choice model. The recommender choice model specifies the probability of a content item k to be recommended for viewer V_i given consideration set \vec{C}_i and treatment allocation \vec{W}_i :

$$\mathbb{P}\left(k_i^* = k \mid V_i, \vec{C}_i, \vec{W}_i; s_0, s_1\right) = \frac{e^{s_0(V_i, C_{i,k}) + W_{i,k} \cdot s_1(V_i, C_{i,k})}}{\sum_{k'=1}^K e^{s_0(V_i, C_{i,k'}) + W_{i,k'} \cdot s_1(V_i, C_{i,k'})}}. \quad (7)$$

The choice model explicitly models interference in the recommendation process. The exposure probability of a content item is affected by not only its own treatment status $W_{i,k}$ but by the treatment status of all items in the same consideration set \vec{W}_i . The recommender choice model serves as the foundation to estimate counterfactual exposure probability under alternative treatment allocation policy, which we describe in detail in Section 3.3.

The recommender choice model is semi-parametric in that it combines the traditional structural choice model with flexible neural nets. Doing so allows us to enjoy the benefits of both. On the one hand, leveraging the choice model enables the treatment effect estimation via counterfactuals under alternative treatment allocations. This would not be feasible with a fully non-parametric black-box model. On the other hand, neural nets can capture flexible relationships so that the

⁸ One alternative model specification is to let the score functions s_0 and s_1 depend not only on the focal content item $C_{i,k}$ but the entire consideration set \vec{C}_i . Under the alternative specification, our modeling and inference framework still apply but the computational cost will significantly increase. We explore this alternative in the Appendix F.

⁹ It is also worth noting that it is impractical to simulate outcomes with “offline” recommender systems. In other words, one cannot simulate recommendations and predict viewer response under treatment or control algorithms respectively (Bennett et al. 2007).

estimated recommender choice model better approximates the behavior of the real-world complex recommender system. Employing neural networks also helps mitigate the independence of irrelevant alternatives (IIA) issue inherent in a standard logit choice model, which results in a proportional substitution pattern. Since neural nets can flexibly account for viewer preferences, adding a new item may disproportionately affect the exposure probability of certain items more than others, depending on content similarity and viewer preferences.

With the score functions parameterized as neural nets, we need an assumption on their boundedness so that the exposure probability of an item is bounded away from zero. In particular, we shall consider universally bounded scores throughout.

ASSUMPTION 2 (Bounded scores). *There exists a universal constant C such that the true score functions are bounded: $\|s_0\|_\infty \leq C$ and $\|s_1\|_\infty \leq C$.*

This assumption is parallel to the “overlap” condition in propensity score-based debiasing methods like AIPW (Imbens 2004). Under this assumption, we show that each item in the consideration set has some positive probability of being recommended, regardless of the treatment assignment. We formalize this by the lemma below. The proof is given in Appendix A.

LEMMA 1. *Under Assumption 2, there exists a universal constant $\delta > 0$ such that each content item in the consideration set has at least δ probability to be recommended:*

$$\mathbb{P}\left(k_i^* = k \mid V_i, \vec{C}_i, \vec{W}_i; s_0, s_1\right) \geq \delta, \quad \forall (V_i, \vec{C}_i, \vec{W}_i, k).$$

Besides enabling ATE estimation, the recommender choice model has standalone practical value for platforms. It represents a model distillation process by summarizing the recommendation pipeline from the consideration set to final item exposure, which can potentially replace the complex existing pipeline to reduce latency when serving viewers online (Tang and Wang 2018). Moreover, the derived “scores” approximate the overall value of recommending content to viewers, skillfully balancing multiple evaluation criteria such as view time, likes, and conversions. These scores can serve as an offline evaluation metric for potential recommender system updates, allowing for preliminary assessments before they are tested in online experiments.

3.2. Viewer Response Model

To complete counterfactual evaluations under alternative treatment allocation, we also need a viewer response model that predicts the viewer response when exposed to an item. The viewer’s response reflects outcomes that the platform is interested in evaluating, such as view time, likes, or conversion rates. We assume the viewer’s response depends on the viewer characteristics V_i and

the characteristics of the exposed content item C_{i,k_i^*} . For an outcome of interest, let the viewer’s response Y_i be:

$$Y_i = z(V_i, C_{i,k_i^*}) + \zeta_i. \quad (8)$$

$z(\cdot, \cdot)$ is a viewer response function that we parameterize as a neural net. It predicts a flexible relationship between the input viewer-content pairs and the outcome. ζ_i is i.i.d. noise. In general, one needs a separate viewer response model for each outcome of interest, but the recommender choice model is commonly shared across different outcomes.

The viewer response model in Eq. (8) assumes that the outcome depends only on the viewer and the exposed item. In particular, it does not depend on the treatment status of the item as long as it is exposed to the viewer. This is a reasonable assumption since viewers are typically not aware of changes in recommendation algorithms. It also assumes that the outcome does not depend on any previous content the viewers may have seen. The model can be extended to allow previous content interactions to enter as input in addition to viewer characteristics, but doing so will lead to a significantly more complex viewer response model.

In practice, platforms typically have pre-existing viewer response predictions from backend algorithms, which is also the case in our empirical context. Thus, we can directly leverage these pre-trained viewer response models and only need to train the recommender choice model. It’s worth noting that our framework does not require an unbiased prediction for these viewer responses. As detailed in Section 5, we introduce a double/debiased estimator with a bias correction term to account for “errors” in the neural net predictions.

3.3. Counterfactual Analysis for Policy Value and Treatment Effect

With the recommender choice model (Eq. 7) and the viewer response model (Eq. 8), we can represent the policy values (Eq. 2) of any counterfactual treatment assignment policy π as follows (see Appendix A.3 for detailed derivation):

$$Q(\pi) = \mathbb{E}_{(V_i, \vec{C}_i, \vec{W}_i \sim \pi)} \left[\sum_{k=1}^K z(V_i, C_{i,k}) \cdot \frac{e^{s_0(V_i, C_{i,k}) + W_{i,k} \cdot s_1(V_i, C_{i,k})}}{\sum_{k'=1}^K e^{s_0(V_i, C_{i,k'}) + W_{i,k'} \cdot s_1(V_i, C_{i,k'})}} \right]. \quad (9)$$

The term in the square bracket captures the expected outcomes of viewer V_i by multiplying the exposure probability and the viewer response conditional on exposure for each item in the consideration set. The policy value $Q(\pi)$ measures the overall outcome by taking the expectation over the distribution of viewer V_i , consideration set \vec{C}_i , and treatment assignment policy \vec{W}_i .

To estimate the treatment effect, we are particularly interested in two specific treatment assignment policies, with all items in the treatment status or all items in the control status. The ATE

(Eq. 3) is the difference between the policy values under global treatment $Q(\pi_1)$ vs. global control $Q(\pi_0)$. Using Eq. (9), the ATE can be written as:

$$\tau = Q(\pi_1) - Q(\pi_0) = \mathbb{E}_{(V_i, \vec{C}_i)} \left[\sum_{k=1}^K z(V_i, C_{i,k}) \cdot \delta_{i,k} \right]. \quad (10)$$

$\delta_{i,k}$ represents the change in the exposure probability for content item $C_{i,k}$ when going from global control to global treatment scenarios. Its explicit expression is provided in Appendix A.1.

Beyond ATE, it is useful for the platform to understand the heterogeneous impact of a new algorithm on different types of creators. It is straightforward to conduct subgroup analysis to estimate heterogeneous treatment effects. For a particular creator/content subgroup \mathcal{C}_0 , the conditional average treatment effect (CATE) can be calculated as:

$$\tau_{\mathcal{C}_0} = \mathbb{E}_{(V_i, \vec{C}_i)} \left[\sum_{k=1}^K I\{C_{i,k} \in \mathcal{C}_0\} \cdot z(V_i, C_{i,k}) \cdot \delta_{i,k} \right]. \quad (11)$$

This is close to Equation (10) except that instead of adding up the expected change in outcomes for all content items in the consideration set, we only do so for the ones that belong in the subgroup of interest, $I\{C_{i,k} \in \mathcal{C}_0\}$.

It is worth noting that with the estimated recommender choice model and viewer response model, it is straightforward to calculate other outcomes of interest beyond the ATE and CATE. As a simple example, although Equation (10) defines the treatment effect as the level difference between treatment and control conditions, $Q(\pi_1) - Q(\pi_0)$. It is just as easy to calculate the treatment effect in relative terms using our framework, $\frac{Q(\pi_1) - Q(\pi_0)}{Q(\pi_0)}$. As a more involved example, our model can also be used to simulate outcomes as the platform scales up the proportion of traffic allocated to the treatment algorithm. In other words, the framework is flexible to account for any treatment assignment policy π beyond the global treatment and global control. We can also leverage the expression in Equation (10) to instantiate Proposition 1 and explicitly characterize the asymptotic bias of the DIM estimator. Details are described in Appendix A.1.

3.4. Scope of the Proposed Approach

By directly modeling the interference pathway through a recommender choice model, the framework captures how one item gets recommended from a consideration set comprised of both treated and control items. Therefore, the proposed approach captures interference in the recommendation phrase that arises from items competing for exposure. Since the proposed approach relies on modeling the exposure probability from a consideration set, it is more applicable to experiments that happen in the later stage of the recommender system (see Section 2.1). In the ranking or re-ranking stages, the size of the consideration set is relatively small. For an experiment that happens in the

early stage (e.g., retrieval stage), it will be intrinsically harder to model exposure from a very large pool of items. Since many recommender experiments involve fine-tuning in the later stages, the proposed approach is applicable to many such experiments in practice.

Our study does not explicitly consider potential viewer-side temporal interference, where viewer responses might be influenced by previous content. For example, suppose the treatment algorithm prioritizes high quality content, viewers may be motivated to stay longer with the platform (hence generating more viewer queries). Viewer responses may also be impacted by prior content because the diversity of recommended content can influence viewer behavior (e.g., novelty effect). Addressing these forms of interference requires more nuanced modeling of viewer behavior, such as using reinforcement learning to model viewer behavior as Markov chain processes to deal with viewer-side temporal interference (Farias et al. 2023).

Our study also abstracts away from the potential long-run effect of the treatment. For example, if a treatment algorithm prioritizes certain types of content, it may create a feedback loop that impacts the content production decisions of different creators. In the long term, it may lead to a different pool of available content on the platform. Addressing this involves modeling the content production decisions based on short-term outcomes (e.g., views and likes) that may vary under different algorithms. Our approach focuses on modeling these short-term outcomes while conditioning on the available content and viewer queries.

4. Estimation and Inference Procedure

In this section, we describe the estimation and inference procedure of the proposed model. We start with the estimation of the neural network components in the recommender choice and viewer response models. We then construct a debiased estimator for treatment effect estimation and inference. Using Monte Carlo simulations, we show that the proposed approach can effectively recover the true point estimate and uncertainty.

4.1. Estimating the Nuisance Components

We start by describing the estimation of the nuisance components in the recommender choice model, which relies on two score functions: s_0 denotes the baseline score and s_1 is the score uplift from the treatment algorithm. Both score functions are parameterized as neural networks.

Recall that for each viewer query i , we observe that viewer V_i with consideration set \vec{C}_i and treatment status \vec{W}_i gets recommended the k_i^{*th} item, C_{i,k_i^*} . Similar to a fully parametric choice model, estimating the choice model with neural networks relies on maximizing the likelihood function or equivalently, minimizing the loss function. The loss function for any $\tilde{s}_0, \tilde{s}_1 \in \mathcal{F}_s$, where \mathcal{F}_s is the function class for s_0 and s_1 , can be written as follows:

$$\ell_1(V_i, \vec{C}_i, \vec{W}_i, k_i^*; \tilde{s}_0, \tilde{s}_1) := -\log \left(\mathbb{P} \left(k_i^* \mid V_i, \vec{C}_i, \vec{W}_i; \tilde{s}_0, \tilde{s}_1 \right) \right) \quad (12)$$

$$= -\left(s_0(V_i, C_{i,k_i^*}) + W_{i,k_i^*} \cdot s_1(V_i, C_{i,k_i^*})\right) + \log\left(\sum_{k=1}^K e^{s_0(V_i, C_{i,k}) + W_{i,k} \cdot s_1(V_i, C_{i,k})}\right).$$

This is commonly known as the cross entropy loss. During the training process, the parameters of the neural networks are updated so that we get the estimated (\hat{s}_0, \hat{s}_1) that minimizes the cross entropy loss:

$$(\hat{s}_0, \hat{s}_1) \in \arg \min_{\hat{s}_0, \hat{s}_1 \in \mathcal{F}_s} \frac{1}{n} \sum_{i=1}^n \ell_1\left(V_i, \vec{C}_i, \vec{W}_i, k_i^*; \tilde{s}_0, \tilde{s}_1\right). \quad (13)$$

Intuitively, the score functions \hat{s}_0 and \hat{s}_1 are learned so that the recommender choice model can best approximate the behavior of the actual recommender system.

We then describe the estimation of the viewer response model. Recall that when viewer V_i gets exposed to content item C_{i,k_i^*} , we observe the outcome Y_i . The role of the viewer response model is to approximate the outcome conditional on the viewer and item pair. This is a standard machine learning task with the loss function determined by the outcome types. For a continuous outcome, the loss function for any $\tilde{z} \in \mathcal{F}_z$, where \mathcal{F}_z is the function class for z , can be written as follows:

$$\ell_2(V_i, C_{i,k_i^*}, Y_i; \tilde{z}) = \left(\tilde{z}(V_i, C_{i,k_i^*}) - Y_i\right)^2. \quad (14)$$

This is commonly known as the mean square error loss. For a categorical outcome, one can use the cross entropy loss. With either type of loss function, we get the estimated \hat{z} by minimizing the loss:

$$\hat{z} \in \arg \min_{\tilde{z} \in \mathcal{F}_z} \frac{1}{n} \sum_{i=1}^n \ell_2(V_i, C_{i,k_i^*}, Y_i; \tilde{z}). \quad (15)$$

We provide a nuisance identification example for a specified parametric model in Appendix C. In practice, the platform often has built prediction models for key outcomes of interest. These model predictions are useful as inputs into the recommendation pipeline since they typically capture key behaviors of interest for the platform, e.g., watch time and likes. In our empirical application (described in Section 5), we directly leverage the platform's existing view response models instead of estimating \hat{z} ourselves.

4.2. Debiased Estimator

We now discuss the estimation and inference procedure for the treatment effect. With the estimated recommender choice model and viewer response model, one can plug in the estimated neural nets $(\hat{s}_0, \hat{s}_1, \hat{z})$ into the ATE formulation in Eq (10) and get a direct plug-in (DPI) estimate. For each observation with viewer and consideration set pair (V_i, \vec{C}_i) , we compute the direct plug-in estimate of ATE μ as:

$$\mu(V_i, \vec{C}_i; \hat{s}_0, \hat{s}_1, \hat{z}) = \sum_{k=1}^K \hat{z}(V_i, C_{i,k}) \left\{ \frac{e^{\hat{s}_0(V_i, C_{i,k}) + \hat{s}_1(V_i, C_{i,k})}}{\sum_{k'=1}^K e^{\hat{s}_0(V_i, C_{i,k'}) + \hat{s}_1(V_i, C_{i,k'})}} - \frac{e^{\hat{s}_0(V_i, C_{i,k})}}{\sum_{k'=1}^K e^{\hat{s}_0(V_i, C_{i,k'})}} \right\}.$$

The direct plug-in (DPI) estimator $\hat{\tau}_n^{DPI}$ is simply the average of these estimates across all observations:

$$\hat{\tau}_n^{DPI} = \frac{1}{n} \sum_{i=1}^n \mu(V_i, \vec{C}_i; \hat{s}_0, \hat{s}_1, \hat{z}). \quad (16)$$

If the components (s_0, s_1, z) are fully parametric, it is straightforward to use the direct plug-in estimator for treatment effect estimation and inference. With these components being neural nets (or other non-parametric models), the direct plug-in estimator is generally not \sqrt{n} -consistent. In particular, $\hat{\tau}_n^{DPI}$ can be biased because of regularization and over-fitting when estimating the nuisances $(\hat{s}_0, \hat{s}_1, \hat{z})$.

Building on the semi-parametric technique (e.g., [Farrell et al. 2020](#)), we introduce a debiased (DB) estimator for treatment effect estimation and inference. The debiased estimator introduces an additional debiasing term to the direct plug-in estimator. For each observation, the debiased estimate ψ is:

$$\begin{aligned} \psi(V_i, \vec{C}_i, \vec{W}_i, k_i^*, Y_i; \hat{s}_0, \hat{s}_1, \hat{z}, \hat{H}) = & \mu(V_i, \vec{C}_i; \hat{s}_0, \hat{s}_1, \hat{z}) \\ & - \nabla \mu(V_i, \vec{C}_i; \hat{s}_0, \hat{s}_1, \hat{z})^T \hat{H}(V_i, \vec{C}_i; \hat{s}_0, \hat{s}_1, \hat{z})^{-1} \nabla \ell(V_i, \vec{C}_i, \vec{W}_i, k_i^*, Y_i; \hat{s}_0, \hat{s}_1, \hat{z}). \end{aligned} \quad (17)$$

The debiased term has three components. The first component $\nabla \mu$ is the gradient of the direct plug-in estimate μ with respect to the nuisances $(\hat{s}_0, \hat{s}_1, \hat{z})$, which captures the sensitivity of the estimate to the nuisance estimation. Let ℓ be the total loss function which combines the loss ℓ_1 from the recommender choice model and ℓ_2 from the viewer response model. The second component \hat{H} estimates the expected Hessian of the loss function ℓ with respect to the nuisances, with the expectation marginalizing over \vec{W}_i under the creator-side randomization. The third component $\nabla \ell$ is the gradient of the loss function ℓ with respect to the nuisances, which is scaled by the curvature of the loss function (the second component). We give the explicit expressions of $(\nabla \mu, H, \nabla \ell)$ in [Appendix B.1](#). The Hessian H is invertible with [Assumption 2](#) (bounded scores). We provide formal results and proofs in [Appendix B.2](#).

The debiased (DB) estimator $\hat{\tau}_n^{DB}$ is the average of ψ across all observations:

$$\hat{\tau}_n^{DB} := \frac{1}{n} \sum_{i=1}^n \psi(V_i, \vec{C}_i, \vec{W}_i, k_i^*, Y_i; \hat{s}_0, \hat{s}_1, \hat{z}, \hat{H}). \quad (18)$$

The debiased estimator $\hat{\tau}_n^{DB}$ satisfies the universal Neyman orthogonality with respect to the nuisances, with formal results provided in [Appendix B.3](#). This property ensures that errors in nuisance estimation impact the treatment effect estimation only to a second-order degree, thereby effectively mitigating bias introduced by inaccuracies in nuisance estimation.

Now we present the main estimation and inference guarantees for the debiased estimator $\hat{\tau}_n^{DB}$. Under mild conditions, we show that $\hat{\tau}_n^{DB}$ is \sqrt{n} -consistent and asymptotically normal. The proof

builds on Chernozhukov et al. (2018), which deals with i.i.d. sample. In our empirical application, however, the data generating process does not yield an i.i.d. sample, even when each viewer query i is treated as independent. This is because for each new observation, if its consideration set overlaps with previous ones, the treatment statuses of the overlapped content items become deterministic. In contrast, for content items without overlap with previous observations, the treatment status for each item follows i.i.d. Bernoulli randomized trials.

THEOREM 1. *Suppose that Assumptions 1 & 2 hold. Assume that the data generating process follows the recommender choice model Equation (7) and the viewer response model Equation (8). Suppose that the nuisance estimates are all bounded by the constant C in Assumption 2 and satisfy the convergence rate: $\|\hat{s}_0 - s_0\|_{L_2} + \|\hat{s}_1 - s_1\|_{L_2} + \|\hat{z} - z\|_{L_2} = o(n^{-1/4})$ and $\|\hat{H} - H\|_{L_2} = o(n^{-1/4})$. Then, the double/debiased estimator $\hat{\tau}_n^{DB}$ in (18) is \sqrt{n} -consistent with $\hat{\tau}_n^{DB} - \tau = O_p(n^{-1/2})$.*

Define the estimated variance as:

$$\hat{V}_n = \frac{1}{n} \sum_{i=1}^n \left(\psi(V_i, \vec{C}_i, \vec{W}_i, k_i^*, Y_i; \hat{s}_0, \hat{s}_1, \hat{z}, \hat{H}) - \hat{\tau}_n^{DB} \right)^2. \quad (19)$$

If \hat{V}_n converges in probability to a constant, then $\hat{\tau}_n^{DB}$ is asymptotically normal with: $\sqrt{n}(\hat{\tau}_n^{DB} - \tau) / \sqrt{\hat{V}_n} \Rightarrow \mathcal{N}(0, 1)$.

The detailed proof for Theorem 1 is provided in Appendix D. At a high level, the proof establishes the asymptotic properties of the debiased estimator $\hat{\tau}_n^{DB}$ by comparing it to an oracle estimator $\tilde{\tau}_n^{DB}$, which assumes the nuisances are known exactly without estimation error. The oracle estimator forms a martingale difference sequence and converges to a normal distribution. Due to Neyman orthogonality, the difference between the debiased estimator and the oracle estimator is shown to be negligible, with this difference bounded effectively.

A common method for estimating nuisance parameters is via cross-fitting/sample-splitting (Chernozhukov et al. 2018, Farrell et al. 2020). However, unlike typical scenarios with i.i.d. samples, our samples may be correlated due to sharing the same items in their consideration sets. As a result, randomly-split folds may not be independent, which could invalidate the proof of validity for the cross-fitted double/debiased estimator Chernozhukov et al. (2018). To address this issue, we can subgroup items in such a way that samples from different groups do not share items in their consideration sets. For example, Viviano (2019) provides an algorithm to achieve this. Alternatively, one may do exhaustive cross-fitting such that for each sample, the estimated nuisances are fitted using all other samples, excluding those that share items in the consideration set. Let K be the number of subgroups, and let nuisances $(\hat{s}_0^{(-k)}, \hat{s}_1^{(-k)}, \hat{z}^{(-k)}, \hat{H}^{(-k)})$ be the estimated nuisances using the $K - 1$

folds excluding group k . Let \mathcal{D}_k collect the data sample in the k -th group. The cross-fitted ATE estimator is given by:

$$\hat{\tau}_n^{DB} = \frac{1}{K} \sum_{k=1}^K \hat{\tau}_n^{(k)}, \quad \text{where} \quad \hat{\tau}_n^{(k)} = \frac{1}{|\mathcal{D}_k|} \sum_{i \in \mathcal{D}_k} \psi \left(V_i, \vec{C}_i, \vec{W}_i, k_i^*, Y_i; \hat{s}_0^{(-k)}, \hat{s}_1^{(-k)}, \hat{z}^{(-k)}, \hat{H}^{(-k)} \right).$$

And the variance of ψ can be estimated as:

$$\hat{V}_n = \frac{1}{K} \sum_{k=1}^K \hat{V}_n^{(k)}, \quad \text{where} \quad \hat{V}_n^{(k)} = \frac{1}{|\mathcal{D}_k|} \sum_{i \in \mathcal{D}_k} (\psi(V_i, \vec{C}_i, \vec{W}_i, k_i^*, Y_i; \hat{s}_0^{(-k)}, \hat{s}_1^{(-k)}, \hat{z}^{(-k)}, \hat{H}^{(-k)}) - \hat{\tau}_n^{DB})^2.$$

With different subgroups independent from each other, the asymptotic properties of this cross-fitted estimator directly inherit those demonstrated in Theorem 1.

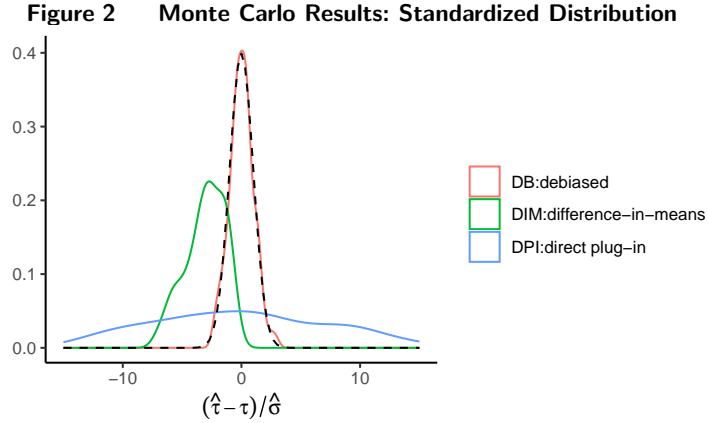
4.3. Monte Carlo Simulations

We use Monte Carlo simulations to validate the estimation and inference results as shown in Theorem 1. We simulate data for $n = 3000$ viewers with $K = 5$ items in the consideration sets that are drawn from a total of $m = 1000$ content items. Each content item has a binary feature (e.g., good vs. bad quality). Every viewer-content pair is associated with a baseline utility score s_0 . The treatment algorithm changes the utility score of bad videos by $\delta = -1.0$. For each viewer i , one video is chosen to be recommended based on the choice model as in (7). The outcome of the chosen video is realized, which is assumed to correlate with the baseline utility score. More details on simulations are described in Appendix G.

We estimate the treatment effects using the proposed debiased (DB) estimator $\hat{\tau}_n^{DB}$ as well as the difference-in-means (DIM) estimator $\hat{\tau}_n^{DIM}$ and the direct plug-in (DPI) estimator $\hat{\tau}_n^{DPI}$. For each of the 100 Monte Carlo datasets, we calculate the point estimate and standard error using each of these estimators. For the DB estimator, the standard error is $n^{-1/2} \hat{V}_n^{1/2}$ as introduced in Theorem 1. We employ 3-fold cross-fitting for nuisance estimation. For the DPI and DIM estimators, the standard errors are calculated as the standard deviation of the sample estimates.¹⁰

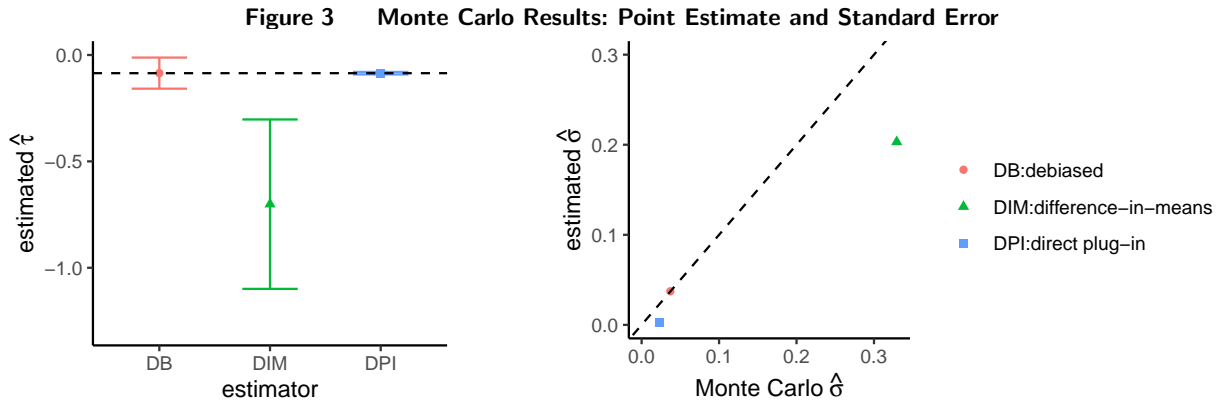
Figure 2 plots the standardized distribution of the estimates from $\hat{\tau}_n^{DB}$, $\hat{\tau}_n^{DIM}$, and $\hat{\tau}_n^{DPI}$. More specifically, we compute the standardized estimates $(\hat{\tau} - \tau)/\hat{\sigma}$, where τ is the true ATE, $\hat{\tau}$ is the point estimate and $\hat{\sigma}$ is the estimated standard error. Essentially, the bias of the estimator is normalized by the estimated standard error. The distribution of these standardized estimates should approximate the standard normal distribution, denoted by the dashed black curve. We see that the distribution from the proposed DB estimator is very close to the standard normal. The DIM estimator has a large bias, and the DPI estimator has a much wider distribution than the standard normal. The simulation results suggest that the proposed DB estimator is unbiased and asymptotically normal, thereby facilitating accurate ATE estimation and inference.

¹⁰ Let $\sigma(a_i)$ denote the sample standard deviation of samples $\{a_i\}$: $\sigma^2(a_i) = n^{-1} \sum_{i=1}^n (a_i - n^{-1} \sum_{i=1}^n a_i)^2$. For the DIM estimator $\hat{\tau}_n^{DIM}$, the standard error estimate is $n^{-1/2} \sigma((W_{k_i^*}/q - (1 - W_{k_i^*})/(1 - q)) Y_i)$. For the DPI estimator $\hat{\tau}_n^{DPI}$, the standard error estimate is $n^{-1/2} \sigma(\mu(V_i, \vec{C}_i; \hat{s}_0, \hat{s}_1, \hat{z}))$.



Note: $(\hat{\tau} - \tau)/\hat{\sigma}$, where $\hat{\tau}$ is the estimate, τ is the true ATE, and $\hat{\sigma}$ is the estimated standard error.

Figure 3 further examines the point estimates and the estimated standard errors. The left panel plots the average point estimates and the 95% confidence intervals, which are computed with the estimated standard errors. Same as shown in Figure 2, the DIM estimator has a large bias. The DPI estimator has a much smaller estimated standard error than the DB estimator. The right panel compares the estimated standard errors with the Monte Carlo standard errors for each estimator, with the 45-degree dashed line. The DB estimator correctly estimates the uncertainty, where the standard errors for both DPI and DIM estimators are underestimated.



5. Empirical Application

This section shows the empirical evidence of our method's effectiveness based on results of a field experiment we implemented on Weixin Channels, a short video platform within Weixin. Benchmarked with an approximated ground truth, we show that our estimator outperforms the standard DIM estimator by providing more accurate ATE estimation.

5.1. Empirical Setting, Experimental Design, and Data

We consider a treatment that affects video exposure during the re-ranking stage in the recommendation pipeline. We implement a unique experimental design combining double-sided and creator-side randomization experiments, creating three separate experimentation worlds: global treatment, global control, and creator-side randomization, as illustrated in Table 1. This design is costly to be implemented at scale but provides a rigorous evaluation of our method.

We maintain an equal market size across these experimentation worlds to mitigate market-size effect. We apply treatment to each simultaneously in both creator-side and double-sided experiments to overcome nonstationarity issues from external factors (e.g., weekends, holidays, weather). In specific, for the creator-side randomization experiment, there are 34,245 videos in the treatment group and control group. For the double-sided randomization experiment, 33,442 videos are in the global control world and 34,021 videos are in the global treatment world. Logged data from Weixin platform of eight days are used for analysis. We omit the number of observations to protect data confidentiality. Our objective is to estimate the ATE and CATE of the treatment on four types of outcomes that reflect viewer’s engagement on the video content.

Particularly, we use the DIM estimates from double-sided randomization as a proxy of the ground truth treatment effect (Bajari et al. 2021, Johari et al. 2022, Ye et al. 2023a). This estimator, referred to as “double-sided DIM”, estimates the treatment effect by contrasting the average outcomes between the global treatment and global control experimentation worlds. We then use data from the creator-side randomization world to assess our double/debiased estimator against the DIM estimator, hereafter called the “creator-side DIM”.

To construct our double/debiased estimation for all four outcomes, we learn a single recommender choice model using data from the creator-side randomization experiment. This choice model is shared across all outcomes. For the nuisance estimation component of the viewer response model, we note that three of these outcomes are related to viewer interactions, for which we utilize the company’s existing prediction model. The fourth outcome is a consumption metric, where the viewer response model assigns a constant value of one to any exposed item; thus for this metric, we do not need to estimate the viewer response but instead know its true value to be one.

5.1.1. Evidence of interference. Our experimentation setup allows us to show empirical evidence of interference by comparing creator-side DIM estimates with double-sided DIM estimates—the latter serving as a reliable approximation of the ATE. When there is no interference, we would expect both DIM estimates to align closely. However, this is contradicted by Table 2, which reveals discrepancies between the two estimators across six key metrics.¹¹ Two of these metrics reflect

¹¹ These metrics differ from those used for treatment effect estimation in Section 5.3 because we lack access to the pairwise viewer response data, which prevents us from estimating the viewer response model and constructing our estimator.

Table 2 Evidence of interference

| | Consumption 1 | Consumption 2 | Interaction 3 |
|------------------|-----------------------------|--------------------------|--------------------------|
| Creator-side DIM | +275.46529 (± 23.594) | +2.99459 (± 0.414) | +0.01347 (± 0.002) |
| Double-sided DIM | +80.56294 (± 30.944) | +0.50240 (± 0.469) | +0.00231 (± 0.002) |
| | Interaction 4 | Interaction 5 | Interaction 6 |
| Creator-side DIM | +0.00417 (± 0.001) | +0.01677 (± 0.002) | +0.00107 (± 0.001) |
| Double-sided DIM | +0.00221 (± 0.002) | +0.00544 (± 0.002) | +0.00156 (± 0.001) |

Note: This table presents DIM estimates and their associated 95% Wald-type confidence intervals for six key metrics, utilizing data from creator-side and blocked double-sided randomization experiments respectively.

viewers’ consumption on videos, while the remaining four measure the interaction rate, which represents the average likelihood of each video exposure leading to an interaction action such as liking, following, or commenting. The creator-side DIM estimator consistently deviates from the double-sided DIM estimator across all metrics, and for some metrics, it even yields estimation outside of the feasible range.

5.2. Fitting the Recommender Choice Model

We now provide details on fitting the recommender choice model, starting with deciding the size of consideration set. Recall that the consideration set should be established before the treatment is applied. A larger consideration set means that more items would interfere with each other and would complicate the computation, as the dimensions of Hessian and gradients in the double/debiased estimator scale with the size of consideration set. To address it, we identify the smallest possible size of pre-treatment consideration set, ensuring that videos outside this set would not be exposed under any treatment assignment. The original collection of videos prior to treatment is ordered by the platform’s internal recommendation algorithms. Figure 4 show that all exposed videos typically rank within the top 15. Based on this observation, we exclude videos ranked 16th or lower, establishing fixed-size consideration sets of $K = 15$.

To fit the choice model, we use neural networks and leverage the existing heuristics generated pre-treatment by the platform’s built-in algorithms. These algorithms already evaluate each viewer-video pair and output scalars. Specifically, for a viewer V_i associated with a video consideration set \vec{C}_i , each heuristic j is represented as $(h_j(V_i, C_{i,1}), \dots, h_j(V_i, C_{i,K}))$. We then feed these heuristics into a two-layer neural network to approximate the score function (s_0, s_1) , as illustrated in Figure 5. We then construct the exposure probability following (7). We use Python’s TensorFlow package to train the model with categorical cross-entropy loss and the Adam optimizer. Figure 6 shows the training loss decay for all 5-folds during the cross-fitting procedure.

5.2.1. Goodness of fit. We now assess how our learned choice model aligns with the actual video exposures in the dataset. We first compare it with a baseline choice model that does not

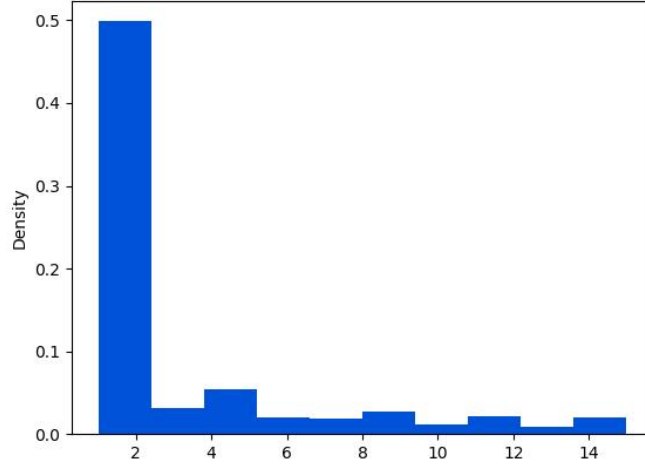


Figure 4 Distribution of ranking of the recommended videos in the consideration set.

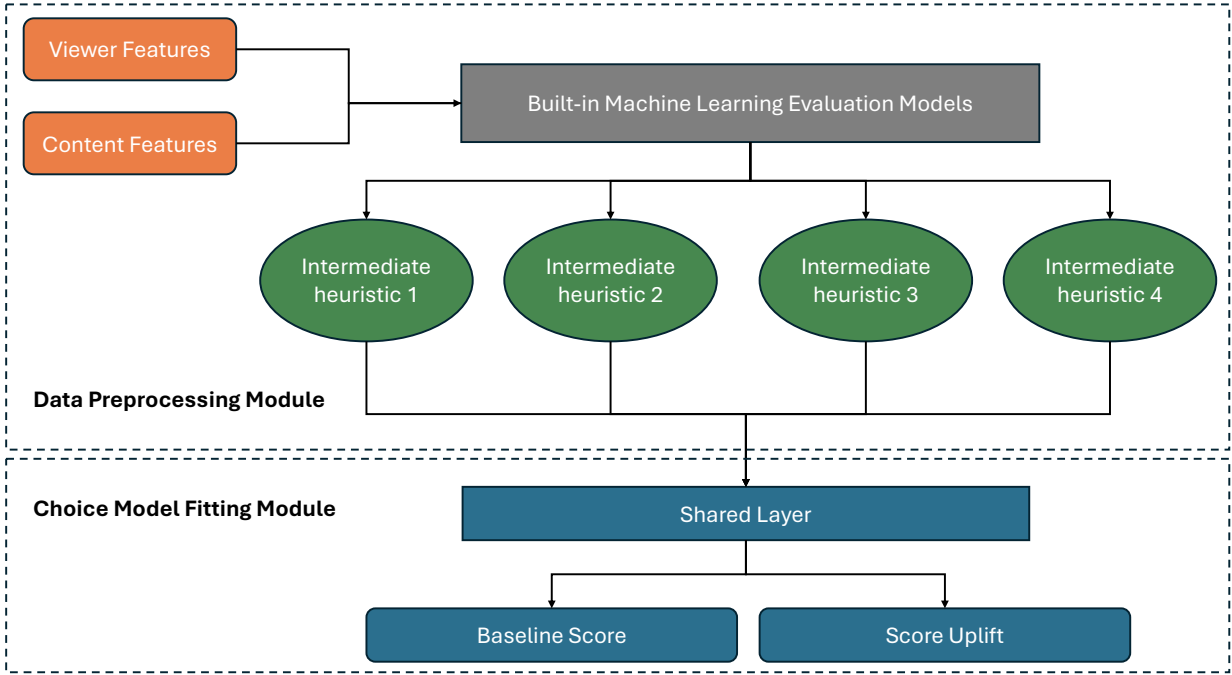


Figure 5 Network structure for fitting the choice model.

use any covariate information. This model assigns the same exposure probability to any viewer, regardless of the consideration set and video treatment statuses. This exposure probability is the marginalized probability aggregated from the creator-side randomization dataset. We perform a likelihood ratio test against the null that the baseline model performs equally as our learned choice model. Note that the baseline model is takes the maximum likelihood estimate for the videos at each position, having degrees of freedom equals to $15 - 1 = 14$. In contrast, our choice model network

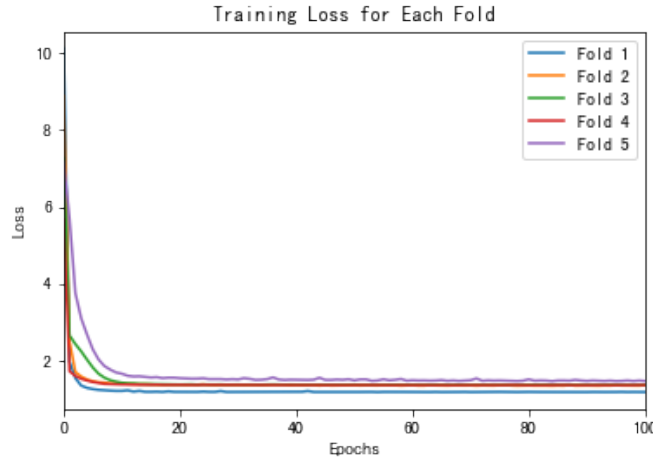


Figure 6 Training loss over the number of training epochs across different folds.

first forwards the 4-dimensional inputs through a common hidden layer of an output of dimension 3, with $4 \times 3 + 3 = 15$ parameters. The output of the common hidden layer is then connected to a baseline logit layer, with $3 \times 1 + 1 = 4$ parameters. Then, for the treatment, a layer for the score uplift has $3 \times 1 + 1 = 4$ parameters. In total, there are $23 - 1 = 22$ parameters, as the baseline logit for the first video in the consideration set is subtracted for the identifiability. Therefore, the degrees of freedom for a χ^2 test comparing the baseline and our learned model is $22 - 14 = 8$. The statistic is 5571, indicating that our learned model performs significantly better than the baseline model.

We next compare our model with a more sophisticated model, termed the “correlated choice model”. In this model, the scores derived for all videos within the consideration set are passed through an additional dense layer before the softmax activation. This extra layer is to capture potential correlations among videos within the same consideration set, addressing interdependencies that our chosen model might ignore.¹² We perform a likelihood ratio test against the null that our choice model performs equally as this more sophisticated model. The degrees of freedom for this comparison are determined by the number of parameters in the additional layer in the Correlated Choice Model, amounting to $15 \times 15 + 15$. With a test statistic of -6701, the χ^2 test did not discover significant difference between our learned choice model and the correlated choice model.

We finally compare all three choice models using two metrics widely used in industry ranking studies: the ROC curve (receiver operating characteristic curve) and NDCG loss (normalized discounted cumulative gain loss) (Valizadegan et al. 2009, Bruch et al. 2019). Figure 7a plots the ROC curve, where our learned model achieves an AUC (area under the curve) of 0.97, indicating a high level of discriminative ability. Figure 7b plots the empirical distribution of the NDCG loss, where

¹² Note that this correlated choice model does not suffer from the IIA condition at the individual level.

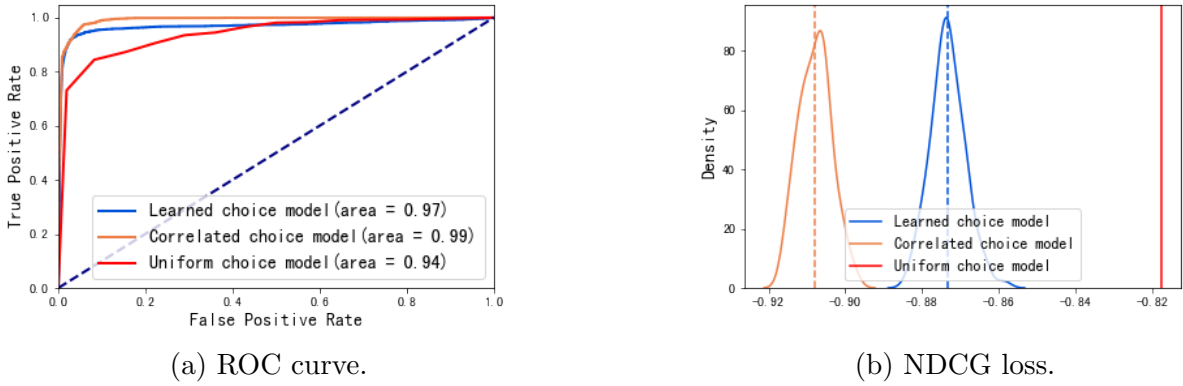


Figure 7 Goodness of fit of learned choice model.

we subsample predicted exposure probabilities against observed exposure vectors. An NDCG loss of -1 indicates perfect alignment, while 0 reflects the least accuracy. Both demonstrate that our learned choice model, which incorporates intermediate heuristics used by the platform’s built-in recommendation pipeline, outperforms the baseline model. Although our modeling framework is not tailored to a specific recommender system, this analysis illustrates an effective way to integrate our choice model with the existing recommender system. By leveraging intermediate heuristics, we can significantly enhance the model’s ability to accurately recover actual video exposures for post-hoc analysis.

5.3. Estimating the Treatment Effects

Below, we compare our debiased estimator with the double-sided DIM (approximated ground truth) and the creator-side DIM (baseline) across four metrics to estimate average treatment effects. Figure 8 presents the ATE estimations for four metrics using all estimators. It shows that our debiased estimator provides more accurate estimation compared to the creator-side DIM estimator, with double-sided DIM estimates serving as a benchmark for the true ATE. The metrics include three binary interaction metrics and one consumption metric. For interaction metric 1, both the double-sided DIM and our debiased estimator indicate insignificant differences, whereas the creator-side DIM suggests a significant positive effect, which is likely erroneous. For the second interaction metric, the creator-side DIM reports a significantly positive effect, in contrast to both the double-sided DIM and our debiased estimator, which identify a significant negative impact on user interaction. For interaction 3, all three estimators align, showing consistent results.

Interestingly, the consumption metric—determined by the internal system’s utility calculation per viewer impression—yields a deterministic outcome of one for exposed videos. Thus the prediction model for this outcome is perfect, leading to a tight confidence interval for our debiased estimator. In practice, within the short-term experimental horizon of our field experiment, the

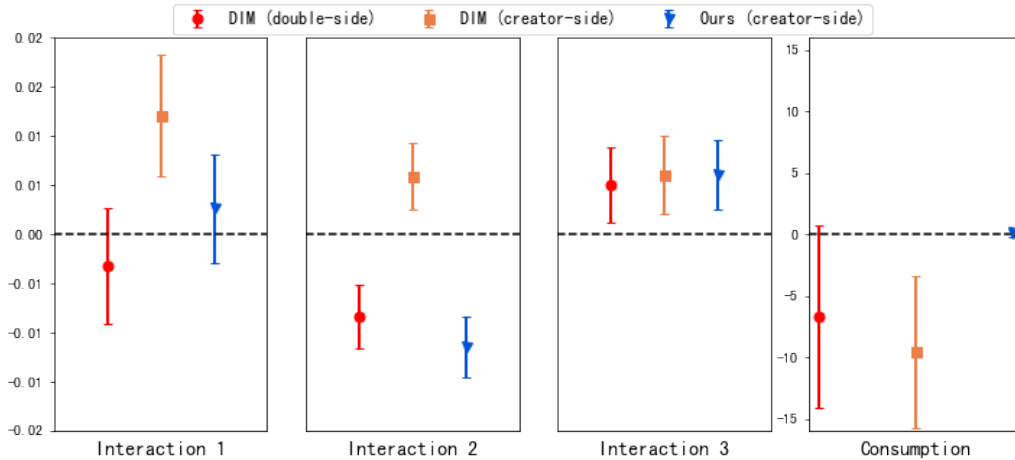


Figure 8 ATE estimation for four metrics.

treatment is unlikely to significantly alter viewer consumption, as viewers’ time and attention are expected to remain stable. This is aligned with the estimations from both the double-sided DIM and our debiased estimator, which indicate an insignificant treatment effect. However, the creator-side DIM estimator shows a negative effect, suggesting it is likely biased.

6. Conclusion

This paper evaluates treatment targeting creators on online content platforms, confronting the challenge of interference in standard creator-side randomization experiments. We demonstrate how such interference can bias ATE estimates using the standard DIM estimator, potentially misrepresenting the effect’s true direction. To address this, we introduce a novel estimator that explicitly models the interference using data from creator-side experiments. This method utilizes a structural choice model to streamline the recommendation process, augmented by nonparametric neural networks to account for the heterogeneity between viewers and content. We show that this estimator achieves consistency and asymptotic normality, supporting hypothesis testing for platform optimization. We evaluate our estimator on a leading short-video platform and show that our approach outperforms DIM estimator in reducing bias and standard error. Future work aims to apply this semiparametric method to broader challenges in online marketplaces, utilizing structural modeling to crystallize market dynamics and machine learning to address heterogeneity.

References

- Aronow PM, Samii C (2017) Estimating average causal effects under general interference, with application to a social network experiment. *The Annals of Applied Statistics* 11(4):1912–1947.
- Bajari P, Burdick B, Imbens GW, Masoero L, McQueen J, Richardson T, Rosen IM (2021) Multiple randomization designs. *arXiv preprint arXiv:2112.13495*.

- Bennett J, Lanning S, et al. (2007) The netflix prize. *Proceedings of KDD cup and workshop*, volume 2007, 35 (New York).
- Bojinov I, Simchi-Levi D, Zhao J (2023) Design and analysis of switchback experiments. *Management Science* 69(7):3759–3777.
- Bright I, Delarue A, Lobel I (2022) Reducing marketplace interference bias via shadow prices. *arXiv preprint arXiv:2205.02274* .
- Bruch S, Zoghi M, Bendersky M, Najork M (2019) Revisiting approximate metric optimization in the age of deep neural networks. *Proceedings of the 42nd international ACM SIGIR conference on research and development in information retrieval*, 1241–1244.
- Cervera MR, Dätwyler R, D’Angelo F, Keurti H, Grewe BF, Henning C (2021) Uncertainty estimation under model misspecification in neural network regression. *arXiv preprint arXiv:2111.11763* .
- Chaney AJ, Stewart BM, Engelhardt BE (2018) How algorithmic confounding in recommendation systems increases homogeneity and decreases utility. *Proceedings of the 12th ACM conference on recommender systems*, 224–232.
- Chernozhukov V, Chetverikov D, Demirer M, Duflo E, Hansen C, Newey W, Robins J (2018) Double/debiased machine learning for treatment and structural parameters. *The Econometrics Journal* 21(1):C1–C68.
- Chernozhukov V, Demirer M, Lewis G, Syrgkanis V (2019) Semi-parametric efficient policy learning with continuous actions. *Advances in Neural Information Processing Systems* 32.
- Covington P, Adams J, Sargin E (2016) Deep neural networks for youtube recommendations. *Proceedings of the 10th ACM conference on recommender systems*, 191–198.
- D’Amour A, Srinivasan H, Atwood J, Baljekar P, Sculley D, Halpern Y (2020) Fairness is not static: deeper understanding of long term fairness via simulation studies. *Proceedings of the 2020 Conference on Fairness, Accountability, and Transparency*, 525–534.
- Dhaouadi W, Johari R, Weintraub GY (2023) Price experimentation and interference in online platforms. *arXiv preprint arXiv:2310.17165* .
- Farias V, Li H, Peng T, Ren X, Zhang H, Zheng A (2023) Correcting for interference in experiments: A case study at douyin. *Proceedings of the 17th ACM Conference on Recommender Systems*, 455–466.
- Farias VF, Li AA, Peng T, Zheng AT (2022) Markovian interference in experiments. *arXiv preprint arXiv:2206.02371* .
- Farrell MH, Liang T, Misra S (2020) Deep learning for individual heterogeneity: An automatic inference framework. *arXiv preprint arXiv:2010.14694* .
- Foster DJ, Syrgkanis V (2023) Orthogonal statistical learning. *The Annals of Statistics* 51(3):879–908.
- Goli A, Lambrecht A, Yoganarasimhan H (2023) A bias correction approach for interference in ranking experiments. *Marketing Science* .

- Ha-Thuc V, Dutta A, Mao R, Wood M, Liu Y (2020) A counterfactual framework for seller-side a/b testing on marketplaces. *Proceedings of the 43rd International ACM SIGIR Conference on Research and Development in Information Retrieval*, 2288–2296.
- Hall P, Heyde CC (2014) *Martingale limit theory and its application* (Academic press).
- Hinton G, Vinyals O, Dean J (2015) Distilling the knowledge in a neural network. *arXiv preprint arXiv:1503.02531* .
- Holtz D, Aral S (2020) Limiting bias from test-control interference in online marketplace experiments. *arXiv preprint arXiv:2004.12162* .
- Holtz D, Brennan J, Pouget-Abadie J (2023a) A study of” symbiosis bias” in a/b tests of recommendation algorithms. *arXiv preprint arXiv:2309.07107* .
- Holtz D, Lobel F, Lobel R, Liskovich I, Aral S (2023b) Reducing interference bias in online marketplace experiments using cluster randomization: Evidence from a pricing meta-experiment on airbnb. *Management Science* .
- Hu Y, Li S, Wager S (2021) Average treatment effects in the presence of interference. *arXiv preprint arXiv:2104.03802* .
- Hu Y, Wager S (2022) Switchback experiments under geometric mixing. *arXiv preprint arXiv:2209.00197* .
- Hudgens MG, Halloran ME (2008) Toward causal inference with interference. *Journal of the American Statistical Association* 103(482):832–842.
- Imbens GW (2004) Nonparametric estimation of average treatment effects under exogeneity: A review. *Review of Economics and statistics* 86(1):4–29.
- Imbens GW, Rubin DB (2015) *Causal Inference in Statistics, Social, and Biomedical Sciences* (Cambridge University Press).
- Ivaniuk A, Duan W (2020) A/b testing at linkedin: Assigning variants at scale. Accessed on Feb 4, 2024. URL <https://www.linkedin.com/blog/engineering/ab-testing-experimentation/a-b-testing-variant-assignment>.
- Johari R, Li H, Liskovich I, Weintraub GY (2022) Experimental design in two-sided platforms: An analysis of bias. *Management Science* 68(10):7069–7089.
- Kiros H (2022) Hated that video? YouTube’s algorithm might push you another just like it. URL <https://www.technologyreview.com/2022/09/20/1059709/youtube-algorithm-recommendations/#:~:text=YouTube’s%20recommendation%20algorithm%20drives%2070,adjust%20what%20it%20shows%20them>.
- Leung MP (2020) Treatment and spillover effects under network interference. *Review of Economics and Statistics* 102(2):368–380.
- Li S, Johari R, Wager S, Xu K (2023) Experimenting under stochastic congestion. *arXiv preprint arXiv:2302.12093* .

- Li S, Wager S (2020) Random graph asymptotics for treatment effect estimation under network interference. *arXiv preprint arXiv:2007.13302* .
- Liang D, Charlin L, McInerney J, Blei DM (2016) Modeling user exposure in recommendation. *Proceedings of the 25th international conference on World Wide Web*, 951–961.
- Ma W, Chen GH (2019) Missing not at random in matrix completion: The effectiveness of estimating missingness probabilities under a low nuclear norm assumption. *Advances in neural information processing systems* 32.
- Mansoury M, Abdollahpouri H, Pechenizkiy M, Mobasher B, Burke R (2020) Feedback loop and bias amplification in recommender systems. *Proceedings of the 29th ACM international conference on information & knowledge management*, 2145–2148.
- Mehrotra R, McInerney J, Bouchard H, Lalmas M, Diaz F (2018) Towards a fair marketplace: Counterfactual evaluation of the trade-off between relevance, fairness & satisfaction in recommendation systems. *Proceedings of the 27th acm international conference on information and knowledge management*, 2243–2251.
- Munro E, Jones D, Brennan J, Nelet R, Mirrokni V, Pouget-Abadie J (2023) Causal estimation of user learning in personalized systems. *arXiv preprint arXiv:2306.00485* .
- Munro E, Wager S, Xu K (2021) Treatment effects in market equilibrium. *arXiv preprint arXiv:2109.11647* .
- Newey WK (1994) The asymptotic variance of semiparametric estimators. *Econometrica: Journal of the Econometric Society* 62(6):1349–1382.
- Newey WK, McFadden D (1994) Chapter 36 large sample estimation and hypothesis testing. volume 4 of handbook of econometrics. *Elsevier* 12:2111–2245.
- Ni T, Bojinov I, Zhao J (2023) Design of panel experiments with spatial and temporal interference. *Available at SSRN 4466598* .
- Rosen S (1981) The economics of superstars. *The American economic review* 71(5):845–858.
- Sävje F, Aronow P, Hudgens M (2021) Average treatment effects in the presence of unknown interference. *Annals of statistics* 49(2):673.
- Schnabel T, Swaminathan A, Singh A, Chandak N, Joachims T (2016) Recommendations as treatments: Debiasing learning and evaluation. *international conference on machine learning*, 1670–1679 (PMLR).
- Si N (2023) Tackling interference induced by data training loops in a/b tests: A weighted training approach. *arXiv preprint arXiv:2310.17496* .
- Sinha A, Gleich DF, Ramani K (2016) Deconvolving feedback loops in recommender systems. *Advances in neural information processing systems* 29.

- Su Y, Wang X, Le EY, Liu L, Li Y, Lu H, Lipshitz B, Badam S, Heldt L, Bi S, et al. (2024) Long-term value of exploration: Measurements, findings and algorithms. *Proceedings of the 17th ACM International Conference on Web Search and Data Mining*, 636–644.
- Sun W, Khenissi S, Nasraoui O, Shafto P (2019) Debiasing the human-recommender system feedback loop in collaborative filtering. *Companion Proceedings of The 2019 World Wide Web Conference*, 645–651.
- Tang J, Wang K (2018) Ranking distillation: Learning compact ranking models with high performance for recommender system. *Proceedings of the 24th ACM SIGKDD international conference on knowledge discovery & data mining*, 2289–2298.
- Taylor S, Wexler J (2003) Where should traffic shaping occur? Accessed on Feb 4, 2024. URL <https://web.archive.org/web/20050207081929/http://www.nwfusion.com/newsletters/frame/2001/00477507.html>.
- Tchetgen EJT, VanderWeele TJ (2012) On causal inference in the presence of interference. *Statistical methods in medical research* 21(1):55–75.
- Train KE (2009) *Discrete choice methods with simulation* (Cambridge university press).
- Ugander J, Karrer B, Backstrom L, Kleinberg J (2013) Graph cluster randomization: Network exposure to multiple universes. *Proceedings of the 19th ACM SIGKDD international conference on Knowledge discovery and data mining*, 329–337.
- Valizadegan H, Jin R, Zhang R, Mao J (2009) Learning to rank by optimizing ndcg measure. *Advances in neural information processing systems* 22.
- Viviano D (2019) Policy targeting under network interference. *arXiv preprint arXiv:1906.10258* .
- Wager S, Xu K (2021) Experimenting in equilibrium. *Management Science* 67(11):6694–6715.
- Wang Y, Ba S (2023) Producer-side experiments based on counterfactual interleaving designs for online recommender systems. *arXiv preprint arXiv:2310.16294* .
- Xiong R, Chin A, Taylor S (2023) Bias-variance tradeoffs for designing simultaneous temporal experiments. *The KDD’23 Workshop on Causal Discovery, Prediction and Decision*, 115–131 (PMLR).
- Ye Z, Zhang DJ, Zhang H, Zhang R, Chen X, Xu Z (2023a) Cold start to improve market thickness on online advertising platforms: Data-driven algorithms and field experiments. *Management Science* 69(7):3838–3860.
- Ye Z, Zhang Z, Zhang D, Zhang H, Zhang RP (2023b) Deep learning based causal inference for large-scale combinatorial experiments: Theory and empirical evidence. *Available at SSRN 4375327* .
- Zhu Z, Cai Z, Zheng L, Si N (2024) Seller-side experiments under interference induced by feedback loops in two-sided platforms. *arXiv preprint arXiv:2401.15811* .

Appendix A: Technical Details for Supporting Results

A.1. Counterfactual Policy Values under Our Model

The ATE under our model can be expressed explicitly as follows.

$$\tau = \mathbb{E} \left[\sum_{k=1}^K z(V_i, C_{i,k}) \cdot \delta_{i,k} \right],$$

$$\text{where } \delta_{i,k} := \frac{e^{s_0(V_i, C_{i,k}) + s_1(V_i, C_{i,k})}}{\sum_{k'=1}^K e^{s_0(V_i, C_{i,k'}) + s_1(V_i, C_{i,k'})}} - \frac{e^{s_0(V_i, C_{i,k})}}{\sum_{k'=1}^K e^{s_0(V_i, C_{i,k'})}}. \quad (20)$$

Our framework also allows us to instantiate Proposition 1 and explicitly characterize the asymptotic bias of DIM estimator:

$$\Delta^{DIM} := \tau^{\mathcal{B}(q)} - \tau = \mathbb{E} \left[\sum_{k=1}^K z(V_i, C_{i,k}) \cdot \left\{ \delta_{i,k}^{\mathcal{B}(q)} - \delta_{i,k} \right\} \right], \quad (21)$$

where $\delta_{i,k}^{\mathcal{B}(q)}$ represents the change in exposure probability for content $C_{i,k}$ due to its own treatment when the treatment statuses for others are sampled from the Bernoulli trial $\mathcal{B}(q)$:

$$\delta_{i,k}^{\mathcal{B}(q)} := \mathbb{E}_{W_{i,k'} \neq k \sim \mathcal{B}(q)} \left[\frac{e^{s_0(V_i, C_{i,k}) + s_1(V_i, C_{i,k})}}{e^{s_0(V_i, C_{i,k}) + s_1(V_i, C_{i,k})} + \sum_{k' \neq k} e^{s_0(V_i, C_{i,k'}) + W_{i,k'} \cdot s_1(V_i, C_{i,k'})}} - \frac{e^{s_0(V_i, C_{i,k})}}{e^{s_0(V_i, C_{i,k})} + \sum_{k' \neq k} e^{s_0(V_i, C_{i,k'}) + W_{i,k'} \cdot s_1(V_i, C_{i,k'})}} \right]. \quad (22)$$

A.2. Proof of Lemma 1

We have

$$\mathbb{P}(k_i^* = k \mid V_i, \vec{C}_i, \vec{W}_i; s_0, s_1) = \frac{e^{s_0(V_i, C_{i,k}) + W_{i,k} \cdot s_1(V_i, C_{i,k})}}{\sum_{k'=1}^K e^{s_0(V_i, C_{i,k'}) + W_{i,k'} \cdot s_1(V_i, C_{i,k'})}} \geq \frac{e^{-2C}}{\sum_{k'=1}^K e^{2C}} = e^{-2C - 2 \log(K)C},$$

where the inequality is by Assumption 2. Set $\delta = e^{-2C - 2 \log(K)C}$, concluding the proof.

A.3. Policy Value under Our Model

We have

$$\begin{aligned} Q(\pi) &= \mathbb{E}_{\mathbf{w} \sim \pi} \left[\sum_{c \in \mathcal{C}} r(c; w_c, \mathbf{w}_{-c}) \right] = \mathbb{E}_{\mathbf{w} \sim \pi} \left[\sum_{c \in \mathcal{C}} \mathbb{E}_v [y(v, c; w_c, \mathbf{w}_{-c})] \right] \\ &= \mathbb{E}_v \left[\mathbb{E}_{\mathbf{w} \sim \pi} \left[\sum_{c \in \mathcal{C}} y(v, c; w_c, \mathbf{w}_{-c}) \right] \right] \\ &= \mathbb{E}_v \left[\mathbb{E}_{\vec{W}_i \sim \pi} \left[Y_i(V_i = v, \vec{C}_i; \vec{W}_i) \right] \right] = \mathbb{E}_{V_i, \vec{W}_i \sim \pi} \left[Y_i(V_i, \vec{C}_i; \vec{W}_i) \right] \\ &= \mathbb{E}_{V_i, \vec{W}_i \sim \pi} \left[\sum_{k=1}^K z(V_i, C_{i,k}) \cdot \mathbb{P}(k_i^* = k \mid V_i, \vec{C}_i, \vec{W}_i) \right] \\ &= \mathbb{E}_{V_i, \vec{W}_i \sim \pi} \left[\sum_{k=1}^K z(V_i, C_{i,k}) \cdot \frac{e^{s_0(V_i, C_{i,k}) + W_{i,k} \cdot s_1(V_i, C_{i,k})}}{\sum_{k'=1}^K e^{s_0(V_i, C_{i,k'}) + W_{i,k'} \cdot s_1(V_i, C_{i,k'})}} \right]. \end{aligned}$$

A.4. Proof of Proposition 1

Let n be the number of recommendations and $m = |\mathcal{C}|$ be the number of content items. Without loss of generality we assume $m = O(n)$, since at most nK contents are considered. Let q be the probability of treatment assignment. For each content c , we use w_c to denote its treatment. The DIM estimator is:

$$\hat{\tau}_n^{DIM} = \frac{1}{nq} \sum_{i=1}^n W_{i,k_i^*} Y_i - \frac{1}{n(1-q)} \sum_{i=1}^n (1 - W_{i,k_i^*}) Y_i.$$

We now characterize the asymptotic behavior of $\hat{\tau}_n^{DIM}$. We have:

$$\begin{aligned}\hat{\tau}_n^{DIM} &= \frac{1}{nq} \sum_{i=1}^n \sum_{c \in \mathcal{C}} w_c \mathbf{1}\{c = C_{i,k_i^*}\} Y_i - \frac{1}{n(1-q)} \sum_{i=1}^n \sum_{c \in \mathcal{C}} (1-w_c) \mathbf{1}\{c = C_{i,k_i^*}\} Y_i \\ &= \frac{1}{nq} \sum_{c \in \mathcal{C}} w_c \sum_{i=1}^n \mathbf{1}\{c = C_{i,k_i^*}\} Y_i - \frac{1}{n(1-q)} \sum_{c \in \mathcal{C}} (1-w_c) \sum_{i=1}^n \mathbf{1}\{c = C_{i,k_i^*}\} Y_i \\ &= \frac{1}{q} \sum_{c \in \mathcal{C}} w_c R_c - \frac{1}{1-q} \sum_{c \in \mathcal{C}} (1-w_c) R_c,\end{aligned}$$

where we use $R_c := \frac{1}{n} \sum_{i=1}^n \mathbf{1}\{c = C_{i,k_i^*}\} Y_i$ to denote the average viewer-outcome for content c . Define:

$$\tau^{\mathcal{B}(q)} = \mathbb{E} \left[\sum_{c \in \mathcal{C}} \{r(c; w_c = 1, \mathbf{w}_{-c} \sim \mathcal{B}(q)) - r(c; w_c = 0, \mathbf{w}_{-c} \sim \mathcal{B}(q))\} \right]$$

We now prove that $\hat{\tau}_n^{DIM}$ converges to $\tau^{\mathcal{B}(q)}$ in probability. Let's first show that $\mathbb{E}[\hat{\tau}_n^{DIM}] = \tau^{\mathcal{B}(q)}$.

$$\begin{aligned}\mathbb{E}[\hat{\tau}_n^{DIM}] &= \sum_{c \in \mathcal{C}} \frac{1}{q} \mathbb{E}_{\mathbf{w} \sim \mathcal{B}(q)}[w_c R_c] - \sum_{c \in \mathcal{C}} \frac{1}{1-q} \mathbb{E}_{\mathbf{w} \sim \mathcal{B}(q)}[(1-w_c) R_c] \\ &= \sum_{c \in \mathcal{C}} \frac{1}{q} \mathbb{E}_{\mathbf{w}_{-c} \sim \mathcal{B}(q)}[R_c | w_c = 1] - \sum_{c \in \mathcal{C}} \frac{1}{1-q} (1-q) \mathbb{E}_{\mathbf{w}_{-c} \sim \mathcal{B}(q)}[R_c | w_c = 0] \\ &= \sum_{c \in \mathcal{C}} \mathbb{E}_{\mathbf{w}_{-c} \sim \mathcal{B}(q)} \left[\frac{1}{n} \sum_{i=1}^n \mathbf{1}\{c = C_{i,k_i^*}\} Y_i | w_c = 1 \right] - \sum_{c \in \mathcal{C}} \mathbb{E}_{\mathbf{w}_{-c} \sim \mathcal{B}(q)} \left[\frac{1}{n} \sum_{i=1}^n \mathbf{1}\{c = C_{i,k_i^*}\} Y_i | w_c = 0 \right] \\ &= \sum_{c \in \mathcal{C}} \mathbb{E}_{\mathbf{w}_{-c} \sim \mathcal{B}(q)} [\mathbf{1}\{c = C_{i,k_i^*}\} Y_i | w_c = 1] - \sum_{c \in \mathcal{C}} \mathbb{E}_{\mathbf{w}_{-c} \sim \mathcal{B}(q)} [\mathbf{1}\{c = C_{i,k_i^*}\} Y_i | w_c = 0] \\ &= \sum_{c \in \mathcal{C}} \mathbb{E}[y(v = V_i, c; w_c = 1, \mathbf{w}_{-c} \sim \mathcal{B}(q))] - \sum_{c \in \mathcal{C}} \mathbb{E}[y(v = V_i, c; w_c = 0, \mathbf{w}_{-c} \sim \mathcal{B}(q))] = \tau^{\mathcal{B}(q)}.\end{aligned}$$

Next let's characterize the variance of $\hat{\tau}_n^{DIM}$. By the law of total variance, we have

$$\text{Var}(\hat{\tau}_n^{DIM}) = \mathbb{E} \left[\text{Var} \left(\hat{\tau}_n^{DIM} \mid \{(V_i, \vec{C}_i)\}_{i=1}^n \right) \right] + \text{Var} \left(\mathbb{E} \left[\hat{\tau}_n^{DIM} \mid \{(V_i, \vec{C}_i)\}_{i=1}^n \right] \right).$$

Conditioning on $\{(V_i, \vec{C}_i)\}_{i=1}^n$, for each content c , we have:

$$\begin{aligned}\text{Var} \left(\frac{w_c R_c}{q} - \frac{(1-w_c) R_c}{1-q} \mid \{(V_i, \vec{C}_i)\}_{i=1}^n \right) &= \frac{\text{Var}(w_c R_c \mid \{(V_i, \vec{C}_i)\}_{i=1}^n)}{q^2} + \frac{\text{Var}((1-w_c) R_c \mid \{(V_i, \vec{C}_i)\}_{i=1}^n)}{(1-q)^2} - \frac{2\text{Cov}(w_c R_c, (1-w_c) R_c \mid \{(V_i, \vec{C}_i)\}_{i=1}^n)}{q(1-q)} \\ &= \frac{\mathbb{E}[w_c^2 R_c^2 \mid \{(V_i, \vec{C}_i)\}_{i=1}^n] - \mathbb{E}[w_c R_c \mid \{(V_i, \vec{C}_i)\}_{i=1}^n]^2}{q^2} + \frac{\mathbb{E}[(1-w_c)^2 R_c^2 \mid \{(V_i, \vec{C}_i)\}_{i=1}^n] - \mathbb{E}[(1-w_c) R_c \mid \{(V_i, \vec{C}_i)\}_{i=1}^n]^2}{(1-q)^2} \\ &\quad + \frac{2\mathbb{E}[w_c R_c \mid \{(V_i, \vec{C}_i)\}_{i=1}^n] \mathbb{E}[(1-w_c) R_c \mid \{(V_i, \vec{C}_i)\}_{i=1}^n]}{q(1-q)} \\ &= \frac{\mathbb{E}[R_c^2 \mid w_c = 1, \{(V_i, \vec{C}_i)\}_{i=1}^n]}{q} - \mathbb{E}[R_c \mid w_c = 1, \{(V_i, \vec{C}_i)\}_{i=1}^n]^2 \\ &\quad + \frac{\mathbb{E}[R_c^2 \mid w_c = 0, \{(V_i, \vec{C}_i)\}_{i=1}^n]}{1-q} - \mathbb{E}[R_c \mid w_c = 0, \{(V_i, \vec{C}_i)\}_{i=1}^n]^2 + 2\mathbb{E}[R_c \mid w_c = 1] \mathbb{E}[R_c \mid w_c = 0, \{(V_i, \vec{C}_i)\}_{i=1}^n] \\ &= \frac{\mathbb{E}[R_c^2 \mid w_c = 1, \{(V_i, \vec{C}_i)\}_{i=1}^n]}{q} + \frac{\mathbb{E}[R_c^2 \mid w_c = 0, \{(V_i, \vec{C}_i)\}_{i=1}^n]}{1-q} - \left(\mathbb{E}[R_c \mid w_c = 1, \{(V_i, \vec{C}_i)\}_{i=1}^n] - \mathbb{E}[R_c \mid w_c = 1, \{(V_i, \vec{C}_i)\}_{i=1}^n] \right)^2\end{aligned}$$

Recall that $R_c := \frac{1}{n} \sum_{i=1}^n \mathbf{1}\{j = k_i^*\} Y_i$. By the boundedness of Y_i and Assumption 1, we have that $R_c =$

$O(\frac{a_n}{n})$, and thus:

$$\text{Var} \left(\frac{w_c R_c}{q} - \frac{(1-w_c) R_c}{1-q} \mid \{(V_i, \vec{C}_i)\}_{i=1}^n \right) = O \left(\frac{a_n^2}{n^2} \right).$$

Also conditioning $\{(V_i, \vec{C}_i)\}_{i=1}^n$, define $I_{c_1, c_2} = 1$ if there exists an item c_3 such that item c_1 and item c_3 present at one consideration set, and item c_2 and item c_3 present at one consideration set simultaneously; otherwise set $I_{c_1, c_2} = 0$. Note that if $I_{c_1, c_2} = 0$, there is no interference among the items c_1 & c_2 and thus R_{c_1} and R_{c_2} independent.

$$\begin{aligned} & \text{Cov}\left(\frac{w_{c_1}R_{c_1}}{q} - \frac{(1-w_{c_1})R_{c_1}}{1-q}, \frac{w_{c_2}R_{c_2}}{q} - \frac{(1-w_{c_2})R_{c_2}}{1-q} \mid \{(V_i, \vec{C}_i)\}_{i=1}^n\right) \\ &= \begin{cases} 0 & \text{if } I_{c_1, c_2} = 0, \\ O\left(\sqrt{\text{Var}\left(\frac{w_{c_1}R_{c_1}}{q} - \frac{(1-w_{c_1})R_{c_1}}{1-q} \mid \{(V_i, \vec{C}_i)\}_{i=1}^n\right)} \sqrt{\text{Var}\left(\frac{w_{c_2}R_{c_2}}{q} - \frac{(1-w_{c_2})R_{c_2}}{1-q} \mid \{(V_i, \vec{C}_i)\}_{i=1}^n\right)}\right) & \text{o.w.} \end{cases} \end{aligned}$$

Together, we have

$$\begin{aligned} \text{Var}\left(\hat{\tau}_n^{DIM} \mid \{(V_i, \vec{C}_i)\}_{i=1}^n\right) &\lesssim \sum_{c \in \mathcal{C}} \text{Var}\left(\frac{w_c R_c}{q} - \frac{(1-w_c)R_c}{1-q} \mid \{(V_i, \vec{C}_i)\}_{i=1}^n\right) \\ &\quad + \sum_{c_1 \neq c_2 \in \mathcal{C}} \text{Cov}\left(\frac{w_{c_1}R_{c_1}}{q} - \frac{(1-w_{c_1})R_{c_1}}{1-q}, \frac{w_{c_2}R_{c_2}}{q} - \frac{(1-w_{c_2})R_{c_2}}{1-q} \mid \{(V_i, \vec{C}_i)\}_{i=1}^n\right) \\ &\lesssim \frac{ma_n^2}{n^2} + \sum_{c_1 \neq c_2 \in \mathcal{C}} I_{c_1, c_2} \frac{a_n^2}{n^2} \lesssim \frac{ma_n^2}{n^2} + \frac{ma_n^4}{n^2} = O\left(\frac{a_n^4}{n}\right). \end{aligned}$$

Thus,

$$\mathbb{E}\left[\text{Var}\left(\hat{\tau}_n^{DIM} \mid \{(V_i, \vec{C}_i)\}_{i=1}^n\right)\right] = O\left(\frac{a_n^4}{n}\right). \quad (23)$$

On the other hand, we have

$$\begin{aligned} \mathbb{E}\left[\hat{\tau}_n^{DIM} \mid \{(V_i, \vec{C}_i)\}_{i=1}^n\right] &= \sum_{c \in \mathcal{C}} \mathbb{E}\left[\frac{1}{n} \sum_{i=1}^n \frac{\mathbf{1}\{c = C_{i, k_i^*}\} w_c}{q} Y_i - \frac{1}{n} \sum_{i=1}^n \frac{\mathbf{1}\{c = C_{i, k_i^*}\} (1-w_c)}{1-q} Y_i \mid \{(V_i, \vec{C}_i)\}_{i=1}^n\right] \\ &= \frac{1}{n} \sum_{i=1}^n \sum_{c \in \mathcal{C}} \left\{ \mathbb{E}\left[\frac{\mathbf{1}\{c = C_{i, k_i^*}\} w_c}{q} Y_i \mid \{(V_i, \vec{C}_i)\}_{i=1}^n\right] - \mathbb{E}\left[\frac{\mathbf{1}\{c = C_{i, k_i^*}\} (1-w_c)}{1-q} Y_i \mid \{(V_i, \vec{C}_i)\}_{i=1}^n\right] \right\} \\ &= \frac{1}{n} \sum_{i=1}^n Z_i, \\ \text{where } Z_i &= \mathbb{E}\left[\left(\frac{W_{i, k_i^*}}{q} - \frac{1-W_{i, k_i^*}}{1-q}\right) Y_i \mid \{(V_i, \vec{C}_i)\}_{i=1}^n\right]. \end{aligned}$$

Note that if sample i_1 and sample i_2 do not share items in the consideration set, i.e., $\vec{C}_{i_1} \cap \vec{C}_{i_2} = \emptyset$, we have $Z_{i_1} \perp Z_{i_2} \mid \{(V_i, \vec{C}_i)\}_{i=1}^n$. Thus,

$$\begin{aligned} \text{Var}\left(\mathbb{E}\left[\hat{\tau}_n^{DIM} \mid \{(V_i, \vec{C}_i)\}_{i=1}^n\right]\right) &= \text{Var}\left(\frac{1}{n} \sum_{i=1}^n Z_i\right) = \frac{\sum_{i=1}^n \text{Var}(Z_i) + \sum_{i_1 \neq i_2} \text{Cov}(Z_{i_1}, Z_{i_2})}{n^2} \\ &= \frac{O(n) + na_n K \cdot O(1)}{n^2} = O\left(\frac{a_n}{n}\right). \end{aligned} \quad (24)$$

Combining (23) & (24), we have

$$\text{Var}\left(\hat{\tau}_n^{DIM}\right) = \mathbb{E}\left[\text{Var}\left(\hat{\tau}_n^{DIM} \mid \{(V_i, \vec{C}_i)\}_{i=1}^n\right)\right] + \text{Var}\left(\mathbb{E}\left[\hat{\tau}_n^{DIM} \mid \{(V_i, \vec{C}_i)\}_{i=1}^n\right]\right) = O\left(\frac{a_n^4}{n}\right) + O\left(\frac{a_n}{n}\right) = O\left(\frac{a_n^4}{n}\right) = o(1).$$

Recall that $\mathbb{E}[\hat{\tau}_n^{DIM}] = \tau^{B(q)}$, by Markov inequality we have

$$\hat{\tau}_n^{DIM} \xrightarrow{P} \tau^{B(q)}. \quad (25)$$

Appendix B: More Results on Double/Debiased Estimator

B.1. Explicit Expression of Debiased Estimation

B.1.1. Debiasing Nuisance Components. We now write out the explicit debiased estimate $\psi(\cdot)$ for each observation, where we drop the subscript i and write the notation as $(V, \vec{C}, \vec{W}, k^*, Y)$ for succinctness. For estimated baseline score function $\hat{s}_0 \in \mathcal{F}_s$, treatment score uplift function $\hat{s}_1 \in \mathcal{F}_s$, and viewer response function $\hat{z} \in \mathcal{F}_z$, we have the estimated exposure probability be

$$\mathbb{P}(k^* = k \mid V, \vec{C}, \vec{W}; \hat{s}_0, \hat{s}_1) = \frac{e^{\hat{s}_0(V, C_k) + W_k \cdot \hat{s}_1(V, C_k)}}{\sum_{k'=1}^K e^{\hat{s}_0(V, C_{k'}) + W_{k'} \cdot \hat{s}_1(V, C_{k'})}} \stackrel{(i)}{=} \frac{e^{\hat{s}_0(V, C_k) - \hat{s}_0(V, C_1) + W_k \cdot \hat{s}_1(V, C_k)}}{\sum_{k'=1}^K e^{\hat{s}_0(V, C_{k'}) - \hat{s}_0(V, C_1) + W_{k'} \cdot \hat{s}_1(V, C_{k'})}},$$

where the equation (i) is obtained by normalizing both the numerator and denominator by the exponential of the first content item's baseline score. In other words, for any baseline score vector $(\hat{s}_0(V, C_1), \hat{s}_0(V, C_2), \dots, \hat{s}_0(V, C_K))$, if we replace it by $(0, \hat{s}_0(V, C_2) - \hat{s}_0(V, C_1), \dots, \hat{s}_0(V, C_K) - \hat{s}_0(V, C_1))$, we will get the same exposure probability result.

This implies that, for any nuisance estimates $(\hat{s}_0, \hat{s}_1, \hat{z})$, the value $\mu(V, \vec{C}; \hat{s}_0, \hat{s}_1, \hat{z})$ can be fully recovered by the vectors

- $\vec{\hat{S}}_0 = (\hat{S}_{0,2}, \dots, \hat{S}_{0,K}) \in \mathbb{R}^{K-1}$ with $\hat{S}_{0,k} = \hat{s}_0(V, C_k) - \hat{s}_0(V, C_1)$;
- $\vec{\hat{S}}_1 = (\hat{S}_{1,1}, \dots, \hat{S}_{1,K}) \in \mathbb{R}^K$ with $\hat{S}_{1,k} = \hat{s}_1(V, C_k)$;
- $\vec{\hat{Z}} = (\hat{Z}_{1,1}, \dots, \hat{Z}_{1,K}) \in \mathbb{R}^K$ with $\hat{Z}_{1,k} = \hat{z}(V, C_k)$.

We thus abuse notations and write $\mu(V, \vec{C}; \vec{\hat{S}}_0, \vec{\hat{S}}_1, \vec{\hat{Z}})$ as $\mu(\vec{\hat{S}}_0, \vec{\hat{S}}_1, \vec{\hat{Z}})$.

The bias of $\mu(\vec{\hat{S}}_0, \vec{\hat{S}}_1, \vec{\hat{Z}})$ comes from the deviation of $(\vec{\hat{S}}_0, \vec{\hat{S}}_1, \vec{\hat{Z}})$ to the true vectors $(\vec{S}_0, \vec{S}_1, \vec{Z})$ that are defined similarly under the true model (s_0, s_1, z) .

We next follow the double machine learning literature and use the outcome (k^*, Y) to correct the bias of $\mu(\vec{\hat{S}}_0, \vec{\hat{S}}_1, \vec{\hat{Z}})$ due to the bias of $(\vec{\hat{S}}_0, \vec{\hat{S}}_1, \vec{\hat{Z}})$ approximating the true $(\vec{S}_0, \vec{S}_1, \vec{Z})$.

Under the estimates $(\vec{\hat{S}}_0, \vec{\hat{S}}_1, \vec{\hat{Z}})$, we reload the loss function notation and write it as:

$$\ell(\vec{W}, k^*, Y; \vec{\hat{S}}_0, \vec{\hat{S}}_1, \vec{\hat{Z}}) = \ell_1(\vec{W}, k^*; \vec{\hat{S}}_0, \vec{\hat{S}}_1) + \ell_2(k^*, Y; \vec{\hat{Z}}),$$

where

$$\ell_1(\vec{W}, k^*; \vec{\hat{S}}_0, \vec{\hat{S}}_1) = \begin{cases} -W_1 \hat{S}_{1,1} + \log \left(e^{W_1 \hat{S}_{1,1}} + \sum_{i=2}^K e^{\hat{S}_{0,k} + W_k \hat{S}_{1,k}} \right) & \text{if } k^* = 1, \\ -(\hat{S}_{0,k} + W_k \hat{S}_{1,k}) + \log \left(e^{W_1 \hat{S}_{1,1}} + \sum_{i=2}^K e^{\hat{S}_{0,k} + W_k \hat{S}_{1,k}} \right) & \text{otherwise;} \end{cases}$$

and

$$\ell_2(k^*, Y; \vec{\hat{Z}}) = (\hat{Z}_{k^*} - Y)^2.$$

We are now ready to introduce the debiased term ψ :

$$\psi(\vec{W}, k^*, Y; \vec{\hat{S}}_0, \vec{\hat{S}}_1, \vec{\hat{Z}}, \hat{H}) = \mu(\vec{\hat{S}}_0, \vec{\hat{S}}_1, \vec{\hat{Z}}) - \nabla \mu^T \hat{H}^{-1} \nabla \ell.$$

Above, $\nabla \mu$ and $\nabla \ell$ are gradients of μ and ℓ with respect to the nuisance estimates $(\vec{\hat{S}}_0, \vec{\hat{S}}_1, \vec{\hat{Z}})$, and \hat{H} estimates the expected Hessian of ℓ regarding $(\vec{\hat{S}}_0, \vec{\hat{S}}_1, \vec{\hat{Z}})$, where the expectation is taken with respect to the treatments \vec{W} that are assigned following the specified creator-side randomization.

B.1.2. Gradient of μ .

Average treatment effect. We have

$$\nabla\mu = \left(\frac{\partial\mu}{\partial\vec{\hat{S}}_0}, \frac{\partial\mu}{\partial\vec{\hat{S}}_1}, \frac{\partial\mu}{\partial\vec{\hat{Z}}} \right)^T = \left(\frac{\partial\mu}{\partial\hat{S}_{0,2}}, \dots, \frac{\partial\mu}{\partial\hat{S}_{0,K}}, \frac{\partial\mu}{\partial\hat{S}_{1,1}}, \dots, \frac{\partial\mu}{\partial\hat{S}_{1,K}}, \frac{\partial\mu}{\partial\hat{Z}_1}, \dots, \frac{\partial\mu}{\partial\hat{Z}_K} \right)^T,$$

where

- for each $k = 2, \dots, K$,

$$\begin{aligned} \frac{\partial\mu}{\partial\hat{S}_{0,k}} &= P(k^* = k; \vec{\hat{S}}_0, \vec{\hat{S}}_1, \vec{W} \equiv 1) \left\{ \hat{Z}_k - \mathbb{E}[Y \mid \vec{\hat{S}}_0, \vec{\hat{S}}_1, \vec{\hat{Z}}, \vec{W} \equiv 1] \right\} \\ &\quad - P(k^* = k; \vec{\hat{S}}_0, \vec{\hat{S}}_1, \vec{W} \equiv 0) \left\{ \hat{Z}_k - \mathbb{E}[Y \mid \vec{\hat{S}}_0, \vec{\hat{S}}_1, \vec{\hat{Z}}, \vec{W} \equiv 0] \right\}. \end{aligned}$$
- for each $k = 1, \dots, K$,

$$\begin{aligned} \frac{\partial\mu}{\partial\hat{S}_{1,k}} &= P(k^* = k; \vec{\hat{S}}_0, \vec{\hat{S}}_1, \vec{W} \equiv 1) \left\{ \hat{Z}_k - \mathbb{E}[Y \mid \vec{\hat{S}}_0, \vec{\hat{S}}_1, \vec{\hat{Z}}, \vec{W} \equiv 1] \right\}, \\ \frac{\partial\mu}{\partial\hat{Z}_k} &= P(k^* = k; \vec{\hat{S}}_0, \vec{\hat{S}}_1, \vec{W} \equiv 1) - P(k^* = k; \vec{\hat{S}}_0, \vec{\hat{S}}_1, \vec{W} \equiv 0). \end{aligned}$$

Above, $\langle \cdot, \cdot \rangle$ denotes inner product between two vectors.

Conditional average treatment effect. Given a subgroup \mathcal{C}_0 , define $J = (\mathbf{1}\{C_{i,1} \in \mathcal{C}_0\}, \dots, \mathbf{1}\{C_{i,K} \in \mathcal{C}_0\})$.

We have

$$\nabla\mu_{\mathcal{C}_0} = \left(\frac{\partial\mu_{\mathcal{C}_0}}{\partial\vec{\hat{S}}_0}, \frac{\partial\mu_{\mathcal{C}_0}}{\partial\vec{\hat{S}}_1}, \frac{\partial\mu_{\mathcal{C}_0}}{\partial\vec{\hat{Z}}} \right)^T = \left(\frac{\partial\mu_{\mathcal{C}_0}}{\partial\hat{S}_{0,2}}, \dots, \frac{\partial\mu_{\mathcal{C}_0}}{\partial\hat{S}_{0,K}}, \frac{\partial\mu_{\mathcal{C}_0}}{\partial\hat{S}_{1,1}}, \dots, \frac{\partial\mu_{\mathcal{C}_0}}{\partial\hat{S}_{1,K}}, \frac{\partial\mu_{\mathcal{C}_0}}{\partial\hat{Z}_1}, \dots, \frac{\partial\mu_{\mathcal{C}_0}}{\partial\hat{Z}_K} \right)^T,$$

where

- for each $k = 2, \dots, K$,

$$\begin{aligned} \frac{\partial\mu_{\mathcal{C}_0}}{\partial\hat{S}_{0,k}} &= P(k^* = k; \vec{\hat{S}}_0, \vec{\hat{S}}_1, \vec{W} \equiv 1) \left\{ \hat{Z}_k \circ J - \langle \hat{Z}_k \circ J, P(\cdot, \vec{\hat{S}}_0, \vec{\hat{S}}_1, \vec{\hat{Z}}, \vec{W} \equiv 1) \rangle \right\} \\ &\quad - P(k^* = k; \vec{\hat{S}}_0, \vec{\hat{S}}_1, \vec{W} \equiv 0) \left\{ \hat{Z}_k \circ J - \langle \hat{Z}_k \circ J, P(\cdot, \vec{\hat{S}}_0, \vec{\hat{S}}_1, \vec{\hat{Z}}, \vec{W} \equiv 0) \rangle \right\}. \end{aligned}$$
- for each $k = 1, \dots, K$,

$$\begin{aligned} \frac{\partial\mu_{\mathcal{C}_0}}{\partial\hat{S}_{1,k}} &= P(k^* = k; \vec{\hat{S}}_0, \vec{\hat{S}}_1, \vec{W} \equiv 1) \left\{ \hat{Z}_k \circ J - \langle \hat{Z}_k \circ J, P(\cdot, \vec{\hat{S}}_0, \vec{\hat{S}}_1, \vec{\hat{Z}}, \vec{W} \equiv 1) \rangle \right\}, \\ \frac{\partial\mu_{\mathcal{C}_0}}{\partial\hat{Z}_k} &= J \cdot \left\{ P(k^* = k; \vec{\hat{S}}_0, \vec{\hat{S}}_1, \vec{W} \equiv 1) - P(k^* = k; \vec{\hat{S}}_0, \vec{\hat{S}}_1, \vec{W} \equiv 0) \right\}. \end{aligned}$$

Above \circ denotes entry-wise product between two vectors.

B.1.3. Gradient of ℓ . We have

$$\nabla\ell = \left(\frac{\partial\ell_1}{\partial\vec{\hat{S}}_0}, \frac{\partial\ell_1}{\partial\vec{\hat{S}}_1}, \frac{\partial\ell_2}{\partial\vec{\hat{Z}}} \right)^T = \left(\frac{\partial\ell_1}{\partial\hat{S}_{0,2}}, \dots, \frac{\partial\ell_1}{\partial\hat{S}_{0,K}}, \frac{\partial\ell_1}{\partial\hat{S}_{1,1}}, \dots, \frac{\partial\ell_1}{\partial\hat{S}_{1,K}}, \frac{\partial\ell_2}{\partial\hat{Z}_1}, \dots, \frac{\partial\ell_2}{\partial\hat{Z}_K} \right)^T,$$

where

- for each $k = 2, \dots, K$:

$$\frac{\partial\ell_1}{\partial\hat{S}_{0,k}} = P(k^* = k; \vec{\hat{S}}_0, \vec{\hat{S}}_1, \vec{W}) - \mathbb{I}[k^* = k].$$
- for each $k = 1, \dots, K$:

$$\begin{aligned} \frac{\partial\ell_1}{\partial\hat{S}_{1,k}} &= \mathbb{I}[W_k = 1] \left(P(k^* = k; \vec{\hat{S}}_0, \vec{\hat{S}}_1, \vec{W}) - \mathbb{I}[k^* = k] \right), \\ \frac{\partial\ell_2}{\partial\hat{Z}_k} &= \mathbb{I}[k^* = k] \left(\hat{Z}_k - Y \right). \end{aligned}$$

B.1.4. Hessian of ℓ . We have

$$\nabla^2 \ell = \begin{pmatrix} \frac{\partial^2 \ell_1}{\partial \hat{S}_0^2} & \frac{\partial^2 \ell_1}{\partial \hat{S}_0 \partial \hat{S}_1} & 0 \\ \frac{\partial^2 \ell_1}{\partial \hat{S}_1 \partial \hat{S}_0} & \frac{\partial^2 \ell_1}{\partial \hat{S}_1^2} & 0 \\ 0 & 0 & \frac{\partial^2 \ell_2}{\partial \hat{Z}^2} \end{pmatrix},$$

where the Hessian of loss function ℓ_1 follows;

$$\begin{aligned} \frac{\partial^2 \ell_1}{\partial \hat{S}_{0,k}^2} &= P(k^* = k; \vec{\hat{S}}_0, \vec{\hat{S}}_1, \vec{W}) \left(1 - P(k^* = k; \vec{\hat{S}}_0, \vec{\hat{S}}_1, \vec{W}) \right), & k \in \{2 : K\} \\ \frac{\partial^2 \ell_1}{\partial \hat{S}_{1,k}^2} &= W_k P(k^* = k; \vec{\hat{S}}_0, \vec{\hat{S}}_1, \vec{W}) \left(1 - P(k^* = k; \vec{\hat{S}}_0, \vec{\hat{S}}_1, \vec{W}) \right), & k \in \{1 : K\} \\ \frac{\partial^2 \ell_1}{\partial \hat{S}_{0,k} \partial \hat{S}_{1,k}} &= W_k P(k^* = k; \vec{\hat{S}}_0, \vec{\hat{S}}_1, \vec{W}) \left(1 - P(k^* = k; \vec{\hat{S}}_0, \vec{\hat{S}}_1, \vec{W}) \right), & k \in \{2 : K\} \\ \frac{\partial^2 \ell_1}{\partial \hat{S}_{0,k_1} \partial \hat{S}_{0,k_2}} &= -P(k^* = k_1; \vec{\hat{S}}_0, \vec{\hat{S}}_1, \vec{W}) P(k^* = k_2; \vec{\hat{S}}_0, \vec{\hat{S}}_1, \vec{W}), & k_1 \neq k_2 \in \{2 : K\} \\ \frac{\partial^2 \ell_1}{\partial \hat{S}_{0,k_1} \partial \hat{S}_{1,k_2}} &= -W_{k_2} P(k^* = k_1; \vec{\hat{S}}_0, \vec{\hat{S}}_1, \vec{W}) P(k^* = k_2; \vec{\hat{S}}_0, \vec{\hat{S}}_1, \vec{W}), & k_1 \neq k_2, k_1 \in \{2 : K\}, k_2 \in \{1 : K\} \\ \frac{\partial^2 \ell_1}{\partial \hat{S}_{1,k_1} \partial \hat{S}_{1,k_2}} &= -W_{k_1} W_{k_2} P(k^* = k_1; \vec{\hat{S}}_0, \vec{\hat{S}}_1, \vec{W}) P(k^* = k_2; \vec{\hat{S}}_0, \vec{\hat{S}}_1, \vec{W}), & k_1 \neq k_2 \in \{1 : K\}. \end{aligned}$$

and the Hessian of loss function ℓ_2 follows:

$$\begin{aligned} \frac{\partial \ell_2^2}{\partial \hat{Z}_k^2} &= \mathbb{I}[k^* = k], & k \in \{1 : K\} \\ \frac{\partial \ell_2^2}{\partial \hat{Z}_{k_1} \partial \hat{Z}_{k_2}} &= 0, & k_1 \neq k_2 \in \{1 : K\}. \end{aligned}$$

B.2. Invertible Hessian

LEMMA 2. Suppose Assumptions 2 hold. Suppose that the estimated scores are bounded: $\|\hat{s}_0\|_\infty \leq C$ and $\|\hat{s}_1\|_\infty \leq C$ for the C in Assumption 2. Under our modeling framework, the expected hessian $H = \mathbb{E} [\nabla^2 \ell | V, \vec{C}]$ is universally invertible with bounded inverse.

Note that H is a two-block diagonal matrix with the first diagonal block being $H_1 := \mathbb{E} [\nabla^2 \ell_1 | V, \vec{C}]$ and the second diagonal block being $H_2 := \mathbb{E} [\nabla^2 \ell_2 | V, \vec{C}]$. It suffices to show that both H_1 and H_2 are universally invertible with bounded inverses.

Regularity of H_1 . Consider the sample (V, \vec{C}, \vec{W}) and estimated nuisance \hat{s}_0, \hat{s}_1 . For notation convenience, we use p_k to represent $P(k^* = k; V, \vec{C}, \vec{W}, \hat{s}_0, \hat{s}_1)$. Define the vector

$$\beta = \begin{pmatrix} p_2 \\ \vdots \\ p_K \\ W_1 p_1 \\ \vdots \\ W_K p_K \end{pmatrix} \in \mathbb{R}^{2K-1},$$

the matrix $A \in \mathbb{R}^{(2K-1) \times (2K-1)}$ with its (K, K) -th entry being $\mathbf{1}[W_1 = 1]p_1$ and others zero and matrix

$$B = \begin{pmatrix} \text{diag}(\sqrt{p_2}, \dots, \sqrt{p_K}) \\ 0, \dots, 0, \\ \text{diag}(\sqrt{p_2} W_2, \dots, \sqrt{p_K} W_K) \end{pmatrix} \in \mathbb{R}^{(2K-1) \times (2K-1)},$$

We thus have

$$H_1 = \mathbb{E} \left[A + BB^T - \beta\beta^T \mid V, \vec{C} \right].$$

We now show that H_1 is positive definite. For any vector $x = (x_1, \dots, x_{2K-1})$ and any treatment assignment \vec{W} , we have

$$\begin{aligned} x^T(A + BB^T - \beta\beta^T)x &= p_1 W_1 x_K^2 + \sum_{j=1}^{K-1} p_{j+1} (x_j + W_{j+1} x_{K+j})^2 - \left(p_1 W_1 x_K + \sum_{j=1}^{K-1} p_{j+1} (x_j + W_{j+1} x_{K+j}) \right)^2 \\ &= \left(p_1 W_1 x_K^2 + \sum_{j=1}^{K-1} p_{j+1} (x_j + W_{j+1} x_{K+j})^2 \right) \left(\sum_{j=1}^K p_j \right) \\ &\quad - \left(p_1 W_1 x_K + \sum_{j=1}^{K-1} p_{j+1} (x_j + W_{j+1} x_{K+j}) \right)^2 \stackrel{(i)}{\geq} 0, \end{aligned} \quad (26)$$

where (i) is by Cauchy-Swartz inequality. That is, for any treatment assignment, the Hessian is positive semi-definite, and thus H_1 (the expected Hessian) is positive semi-definite.

We next consider specific assignments of \vec{W} to lower bound the smallest eigenvalue of H_1 . Also note that under the assumption of the boundedness of score functions, there exists a constant $\delta > 0$, such that for any $(U, \vec{V}, \vec{W}, k^*)$, we have $P(k^* \mid U, \vec{V}, \vec{W}, \hat{s}_0, \hat{s}_1) \geq \delta$.

Consider $\vec{W}^{(a)} = (0, \dots, 0)$. Then we have (26) instantiate as

$$\begin{aligned} x^T(A + BB^T - \beta\beta^T)x &= \sum_{j=1}^{K-1} p_{j+1}^{(a)} x_j^2 - \left(\sum_{j=1}^{K-1} p_{j+1}^{(a)} x_j \right)^2 \\ &= p_1^{(a)} \sum_{j=1}^{K-1} p_{j+1}^{(a)} x_j^2 + \left(\sum_{j=1}^{K-1} p_{j+1}^{(a)} \right) \sum_{j=1}^{K-1} p_{j+1}^{(a)} x_j^2 - \left(\sum_{j=1}^{K-1} p_{j+1}^{(a)} x_j \right)^2 \geq p_1 \sum_{j=1}^{K-1} p_{j+1}^{(a)} x_j^2 \geq \delta^2 \sum_{j=1}^{K-1} x_j^2, \end{aligned} \quad (27)$$

where the last inequality is due to Cauchy-Schwartz inequality.

Consider $\vec{W}^{(b)} = (0, 1, \dots, 1)$. Then we have (26) instantiate as

$$\begin{aligned} x^T(A + BB^T - \beta\beta^T)x &= \sum_{j=1}^{K-1} p_{j+1}^{(b)} (x_j + x_{K+j})^2 - \left(\sum_{j=1}^{K-1} p_{j+1}^{(b)} (x_j + x_{K+j}) \right)^2 \\ &= p_1^{(b)} \sum_{j=1}^{K-1} p_{j+1}^{(b)} (x_j + x_{K+j})^2 + \left(\sum_{j=1}^{K-1} p_{j+1}^{(b)} \right) \sum_{j=1}^{K-1} p_{j+1}^{(b)} (x_j + x_{K+j})^2 - \left(\sum_{j=1}^{K-1} p_{j+1}^{(b)} (x_j + x_{K+j}) \right)^2 \\ &\stackrel{(i)}{\geq} p_1^{(b)} \sum_{j=1}^{K-1} p_{j+1}^{(b)} (x_j + x_{K+j})^2 \geq \delta^2 \sum_{j=1}^{K-1} (x_j + x_{K+j})^2 = \delta^2 \sum_{j=1}^{K-1} (x_j^2 + x_{K+j}^2 + 2x_j x_{K+j}) \\ &\stackrel{(ii)}{\geq} \delta^2 \sum_{j=1}^{K-1} (x_j^2 + x_{K+j}^2 - \frac{2}{3} x_{K+j}^2 - \frac{3}{2} x_j^2) = \delta^2 \sum_{j=1}^{K-1} \left(-\frac{1}{2} x_j^2 + \frac{1}{3} x_{K+j}^2 \right), \end{aligned} \quad (28)$$

where both (i) and (ii) are due to Cauchy-Schwartz inequality.

Consider $\vec{W}^{(c)} = (1, 0, \dots, 0)$. We have (26) instantiate as

$$x^T(A + BB^T - \beta\beta^T)x = p_1^{(c)} x_K^2 + \sum_{j=1}^{K-1} p_{j+1}^{(c)} x_j^2 - \left(p_1^{(c)} x_K + \sum_{j=1}^{K-1} p_{j+1}^{(c)} x_j \right)^2 \quad (29)$$

Note that under creator-side randomization, each \vec{W} has assignment probability bounded away from zero, and we denote this lower bound as $\eta > 0$. Also recall that each item exposure probability is lower bounded by $\delta > 0$, with $K\delta \leq 1$. Combining (27), (28), (29), with the fact that the Hessian for any \vec{W} is semi-definite, we have

$$\begin{aligned}
 x^T H_1 x &= \mathbb{E}[x^T (A + BB^T - \beta\beta^T) | V, \vec{C}] \\
 &\geq P(\vec{W} = \vec{W}^{(a)}) \delta^2 \sum_{j=1}^{K-1} x_j^2 + P(\vec{W} = \vec{W}^{(b)}) \delta^2 \sum_{j=1}^{K-1} \left\{ -\frac{1}{2}x_j^2 + \frac{1}{3}x_{K+j}^2 \right\} \\
 &\quad + P(\vec{W} = \vec{W}^{(c)}) \left\{ p_1^{(c)} x_K^2 + \sum_{j=1}^K p_{j+1}^{(c)} x_j^2 - \left(p_1^{(c)} x_K + \sum_{j=1}^{K-1} p_{j+1}^{(c)} x_j \right)^2 \right\} \\
 &\geq \eta \delta^2 \sum_{j=1}^{K-1} x_j^2 + \frac{\eta \delta^2}{2} \sum_{j=1}^{K-1} \left\{ -\frac{1}{2}x_j^2 + \frac{1}{3}x_{K+j}^2 \right\} + \frac{\eta \delta^2}{2(1-(K-1)\delta)^2} \left\{ p_1^{(c)} x_K^2 + \sum_{j=1}^K p_{j+1}^{(c)} x_j^2 - \left(p_1^{(c)} x_K + \sum_{j=1}^{K-1} p_{j+1}^{(c)} x_j \right)^2 \right\} \\
 &= \frac{\eta \delta^2}{2} \sum_{j=1}^{K-1} \left\{ \frac{1}{2}x_j^2 + \frac{1}{3}x_{K+j}^2 \right\} + I,
 \end{aligned} \tag{30}$$

where $I = \frac{\eta \delta^2}{2(1-(K-1)\delta)^2} \left\{ p_1^{(c)} x_K^2 + \sum_{j=1}^{K-1} (p_{j+1}^{(c)} + (1-(K-1)\delta)^2) x_j^2 - \left(p_1^{(c)} x_K + \sum_{j=1}^{K-1} p_{j+1}^{(c)} x_j \right)^2 \right\}$. We next lower bound term I.

$$\begin{aligned}
 I &\geq \frac{\eta \delta^2}{2(1-(K-1)\delta)^2} \left\{ p_1^{(c)} x_K^2 + \sum_{j=1}^{K-1} (1+p_1^{(c)}) p_{j+1}^{(c)} x_j^2 - \left(p_1^{(c)} x_K + \sum_{j=1}^{K-1} p_{j+1}^{(c)} x_j \right)^2 \right\} \\
 &= \frac{\eta \delta^2}{2(1-(K-1)\delta)^2} \left\{ \left(p_1^{(c)} x_K^2 + \sum_{j=1}^{K-1} (1+p_1^{(c)}) p_{j+1}^{(c)} x_j^2 \right) \left(p_1^{(c)} + \sum_{j=1}^{K-1} \frac{p_{j+1}^{(c)}}{1+p_1^{(c)}} + \frac{p_1^{(c)} - (p_1^{(c)})^2}{p_1^{(c)} + 1} \right) - \left(p_1^{(c)} x_K + \sum_{j=1}^{K-1} p_{j+1}^{(c)} x_j \right)^2 \right\} \\
 &\stackrel{(i)}{\geq} \frac{\eta \delta^2}{2(1-(K-1)\delta)^2} \left(p_1^{(c)} x_K^2 + \sum_{j=1}^{K-1} (1+p_1^{(c)}) p_{j+1}^{(c)} x_j^2 \right) \left(\frac{p_1^{(c)} - (p_1^{(c)})^2}{p_1^{(c)} + 1} \right) \\
 &\geq \frac{\eta \delta^2}{2(1-(K-1)\delta)^2} \left(p_1^{(c)} x_K^2 + \sum_{j=1}^{K-1} (1+p_1^{(c)}) p_{j+1}^{(c)} x_j^2 \right) \frac{p_1^{(c)}(1-p_1^{(c)})}{2} \\
 &\geq \frac{\eta \delta^2 (p_1^{(c)})^2 (1-p_1^{(c)})}{4(1-(K-1)\delta)^2} x_K^2 \geq \frac{\eta \delta^5}{4(1-(K-1)\delta)^2} x_K^2,
 \end{aligned} \tag{31}$$

where (i) is by Cauchy-Schwarz. Putting (30) and (31) together, for any $x = (x_1, \dots, x_{2K-1})$, we have

$$x^T H_1 x \geq \frac{\eta \delta^2}{2} \sum_{j=1}^{K-1} \left\{ \frac{1}{2}x_j^2 + \frac{1}{3}x_{K+j}^2 \right\} + \frac{\eta \delta^5}{4(1-(K-1)\delta)^2} x_K^2. \tag{32}$$

Therefore, H_1 has the smallest eigenvalue of greater than or equal to $\frac{\eta \delta^2}{2} \min\left(\frac{1}{3}, \frac{\delta^3}{2(1-(K-1)\delta)^2}\right)$ and thus is invertible with bounded inverse.

Regularity of H_2 . We have H_2 is a diagonal matrix with its k -th diagonal entry being

$$H_2(k, k) = \mathbb{E} \left[\mathbb{E} \left[P(k^* = k | U, \vec{V}, \vec{W}, \hat{s}_0, \hat{s}_1) \right] | U, \vec{V} \right] \geq \delta.$$

As a result, $H_2 \geq \delta \cdot I$ and thus is invertible with bounded inverse.

B.3. Universal Neyman Orthogonality

We show that the debiased estimate ψ , defined in (17), satisfies the universal Neyman orthogonality (Chernozhukov et al. 2019, Foster and Syrgkanis 2023). This property means that the nuisance estimation error only has a second order effect on the debiased estimate – a key property for achieving the asymptotic normality of the debiased estimator.

PROPOSITION 2 (Universal Orthogonality). *The debiased estimator ψ defined in (17) is universally orthogonal with respect to the nuisances in the sense that, for any nuisance components $(\tilde{s}_0, \tilde{s}_1, \tilde{z}, \tilde{H})$,*

$$\mathbb{E}[\nabla\psi(V, \vec{C}, \vec{W}, k^*, Y; \tilde{s}_0 = s_0, \tilde{s}_1 = s_1, \tilde{z} = z, \tilde{H} = H) \mid V, \vec{C}] = 0,$$

where $(V, \vec{C}, \vec{W}, k^*, Y)$ is sampled from the creator-side randomization experiment, and $\nabla\psi$ is the gradient with respect to the nuisances.

Recall that

$$\begin{aligned} \psi(V, \vec{C}, \vec{W}, k^*, Y; \tilde{s}_0, \tilde{s}_1, \tilde{z}, \tilde{H}) &= \mu(V, \vec{C}; \tilde{s}_0, \tilde{s}_1, \tilde{z}) \\ &\quad - \nabla\mu(V, \vec{C}; \tilde{s}_0, \tilde{s}_1, \tilde{z})^T \tilde{H}(V, \vec{C}; \tilde{s}_0, \tilde{s}_1, \tilde{z})^{-1} \nabla\ell(V, \vec{C}, \vec{W}, k^*, Y; \tilde{s}_0, \tilde{s}_1, \tilde{z}), \end{aligned}$$

Let $\tilde{h} = (\tilde{s}_0, \tilde{s}_1, \tilde{z}, \tilde{H}^{-1})$ with the ground truth $h = (s_0, s_1, z, H^{-1})$. It suffices to show that

$$\mathbb{E}[\nabla_{\tilde{h}}\psi(V, \vec{C}, \vec{W}, k^*, Y; \tilde{h} = h) \mid V, \vec{C}] = 0.$$

We have

$$\begin{aligned} \frac{\partial\psi(\tilde{h} = h)}{\partial(\tilde{s}_0, \tilde{s}_1, \tilde{z})} &= \nabla\mu(V, \vec{C}; s_0, s_1, z) - \nabla^2\mu(V, \vec{C}; s_0, s_1, z)H(V, \vec{C}; s_0, s_1, z)^{-1} \nabla\ell(V, \vec{C}, \vec{W}, k^*, Y; s_0, s_1, z) \\ &\quad - \nabla\mu(V, \vec{C}; s_0, s_1, z)H(V, \vec{C}; s_0, s_1, z)^{-1} \nabla^2\ell(V, \vec{C}, \vec{W}, k^*, Y; s_0, s_1, z). \end{aligned}$$

Then taking the expectation with respect to (\vec{W}, k^*, Y) , we have

$$\begin{aligned} \mathbb{E}\left[\frac{\partial\psi(\tilde{h} = h)}{\partial(\tilde{s}_0, \tilde{s}_1, \tilde{z})} \mid V, \vec{C}\right] &= \nabla\mu(V, \vec{C}; s_0, s_1, z) \left(I - H(V, \vec{C}; s_0, s_1, z)^{-1} \mathbb{E}\left[\nabla^2\ell(V, \vec{C}, \vec{W}, k^*, Y; s_0, s_1, z) \mid V, \vec{C}\right] \right) \\ &\quad - \nabla^2\mu(V, \vec{C}; s_0, s_1, z)H(V, \vec{C}; s_0, s_1, z)^{-1} \mathbb{E}\left[\nabla\ell(V, \vec{C}, \vec{W}, k^*, Y; s_0, s_1, z) \mid V, \vec{C}\right] \\ &\stackrel{(i)}{=} \nabla\mu(V, \vec{C}; s_0, s_1, z) \left(I - H(V, \vec{C}; s_0, s_1, z)^{-1} H(V, \vec{C}; s_0, s_1, z) \right) = 0, \end{aligned}$$

where (i) is because the ground truth (s_0, s_1, z) satisfies the first-order optimality condition of loss function ℓ . Similarly, we have

$$\mathbb{E}\left[\frac{\partial\psi(\tilde{h} = h)}{\partial(\tilde{H}^{-1})} \mid V, \vec{C}\right] = -\mathbb{E}\left[\nabla\ell(V, \vec{C}, \vec{W}, k^*, Y; s_0, s_1, z) \mid V, \vec{C}\right] \nabla\mu(V, \vec{C}; s_0, s_1, z)^T = 0.$$

B.4. Asymptotic Normality

We prove the below theorem to show the asymptotic normality of our debiased estimator.

THEOREM 1. *Suppose that Assumptions 1 & 2 hold. Assume that the data generating process follows the recommender choice model Equation (7) and the viewer response model Equation (8). Suppose that the nuisance estimates are all bounded by the constant C in Assumption 2 and satisfy the convergence rate: $\|\hat{s}_0 - s_0\|_{L_2} + \|\hat{s}_1 - s_1\|_{L_2} + \|\hat{z} - z\|_{L_2} = o(n^{-1/4})$ and $\|\hat{H} - H\|_{L_2} = o(n^{-1/4})$. Then, the double/debiased estimator $\hat{\tau}_n^{DB}$ in (18) is \sqrt{n} -consistent with $\hat{\tau}_n^{DB} - \tau = O_p(n^{-1/2})$.*

Define the estimated variance as:

$$\hat{V}_n = \frac{1}{n} \sum_{i=1}^n \left(\psi(V_i, \vec{C}_i, \vec{W}_i, k_i^*, Y_i; \hat{s}_0, \hat{s}_1, \hat{z}, \hat{H}) - \hat{\tau}_n^{DB} \right)^2. \quad (19)$$

If \hat{V}_n converges in probability to a constant, then $\hat{\tau}_n^{DB}$ is asymptotically normal with: $\sqrt{n}(\hat{\tau}_n^{DB} - \tau) / \sqrt{\hat{V}_n} \Rightarrow \mathcal{N}(0, 1)$.

We shall adapt Theorem 3 from Farrell et al. (2020) to our setting and demonstrate that all requisite conditions specified therein are satisfied. Specifically, we focus on verifying their Assumption 4, reformulated within our context as follows:

- (i) The nuisance components (s_0, s_1, z) are identified by $\arg \min_{\tilde{s}_0, \tilde{s}_1, \tilde{z}} \mathbb{E}[\ell(V, \vec{C}, \vec{W}, k^*, Y) | \tilde{s}_0, \tilde{s}_1, \tilde{z}]$, where $\ell(\cdot)$ is thrice continuously differentiable with respect to the nuisances.
- (ii) The true nuisances satisfy the first-order condition: $\mathbb{E}[\nabla \ell(V, \vec{C}, \vec{W}, k^*, Y) | s_0, s_1, z] = 0$.
- (iii) The expected Hessian $H(V, \vec{C})$ is universally invertible with bounded inverse.
- (iv) The average treatment effect τ is identified and pathwise differentiable and the direct estimator μ is thrice continuously differentiable in nuisances.
- (v) μ and $\nabla \ell$ have $q > 4$ finite absolute moments and positive variance.

Conditions (i), (ii), (iii), and (v) are directly satisfied within our model framework. The key condition is Condition (iv), which requires the expected Hessian to be universally invertible—a result that has been shown in Lemma 2, with the detailed proof available in Appendix B.2.

Appendix C: Discussion on Identifying Nuisances

We now provide more details on the identifiability of the nuisance components. At a high level, these nuisances can be well estimated if we have a personalized recommender system, as the case for our empirical application. To crystallize this idea, let's consider a concrete example where the score functions are parameterized as follows:

$$s_0(U_i, C_{i,k}) = \beta_0^T \psi(V_i, C_{i,k}) \quad \text{and} \quad s_1(U_i, C_{i,k}) = \beta_1^T \psi(V_i, C_{i,k}). \quad (33)$$

Above, $\psi(\cdot)$ is some feature mapping function we shall discuss shortly, and β_0, β_1 are the score coefficient vectors we want to identify using the data from a creator-side randomization experiment. With that, the original identification problem (13) is equivalent to the following:

$$\hat{\beta}_0, \hat{\beta}_1 \in \arg \min_{\tilde{\beta}_0, \tilde{\beta}_1} \mathcal{L}_1(\tilde{\beta}_0, \tilde{\beta}_1) := \frac{1}{n} \sum_{i=1}^n \ell_1 \left(V_i, \vec{C}_i, \vec{W}_i, C_i^*, Y_i; \tilde{\beta}_0, \tilde{\beta}_1 \right), \quad (34)$$

where $\ell_1(\cdot)$ is the cross-entropy loss defined in (12). As a result, $(\hat{\beta}_0, \hat{\beta}_1)$ is the maximum likelihood estimation (MLE). Assuming that the covariance matrix, defined as follows,

$$\Sigma := \mathbb{E}[X_i X_i^\top], \quad \text{where } X_i = (\psi(V_i, C_{i,1}); \dots; \psi(V_i, C_{i,K})), \quad (35)$$

has bounded inverse. Then under mild conditions, this MLE is asymptotically normal (Newey and McFadden 1994):

$$\sqrt{n}(\hat{\beta}_0 - \beta_0) \xrightarrow{d} \mathcal{N}(0, \mathcal{I}_0^{-1}) \quad \text{and} \quad \sqrt{n}(\hat{\beta}_1 - \beta_1) \xrightarrow{d} \mathcal{N}(0, \mathcal{I}_1^{-1}) \quad (36)$$

where $\mathcal{I}_0 = \mathbb{E}[\frac{\partial^2 \ell_1(\tilde{\beta}_0)}{(\partial \tilde{\beta}_0)^2} \mid \tilde{\beta}_0 = \beta_0]$ and $\mathcal{I}_1 = \mathbb{E}[\frac{\partial^2 \ell_1(\tilde{\beta}_1)}{(\partial \tilde{\beta}_1)^2} \mid \tilde{\beta}_1 = \beta_1]$ are the Fisher information matrices that measure the amount of information data carries to identify the parameter vectors β_0 and β_1 respectively. The regularities of \mathcal{I}_0 and \mathcal{I}_1 are determined by the regularity of Σ , as formalized by the result below.

LEMMA 3. *Suppose Assumption 2 holds, and thus there exists a universal constant $\delta > 0$ that lower bounds the item exposure probability by Lemma 1. Suppose the content exposure follows the recommender choice model Eq.(7), with the score form specified in (33). Consider data has been collected from a creator-side randomization experiment with treated probability $q \in (0, 1)$. Suppose that the covariate matrix Σ in (35) satisfies that*

$$c \cdot I \preceq \Sigma \preceq C \cdot I,$$

for positive constants c, C . Then, the Fisher information matrices $\mathcal{I}_0, \mathcal{I}_1$ in (36) satisfies:

$$\delta^2 c K(K-1) \cdot I \preceq \mathcal{I}_0 \preceq C K(K-1) I, \quad \delta^2 q c K(K-1) \cdot I \preceq \mathcal{I}_1 \preceq q C K(K-1) \cdot I.$$

Therefore, the identifiability of β_0 and β_1 depends on the regularity of the covariate matrix Σ , which is typically well-conditioned in many contexts, including ours, where the recommendation process is highly personalized. This personalization ensures that the covariate X_i varies significantly among viewers V_i , leading to $\Sigma = \mathbb{E}[X_i X_i^\top]$ being full-rank with bounded inverse. Furthermore, the identifiability of β_1 also depends on the treatment randomization probability q , with its estimation variance scaling with q^{-1} (also known as inverse propensity), consistent with causal inference literature.

C.1. Proof of Lemma 3

Write $X_{i,k} = \psi(V_i, C_{i,k})$, and $P_{i,k} = \mathbb{P}(k = k^* \mid V_i, \vec{C}_i, \vec{W}_i, C_i^*; s_0, s_1)$. We have

$$\begin{aligned} \frac{\partial \ell_1(V_i, \vec{C}_i, \vec{W}_i, C_i^*, Y_i)}{\partial \beta_0} &= \sum_{i=1}^K \mathbf{1}\{k = k^*\} (-X_{i,k}) + \sum_{k=1}^K P_{i,k} X_{i,k}, \\ \frac{\partial \ell_1(V_i, \vec{C}_i, \vec{W}_i, C_i^*, Y_i)}{\partial \beta_1} &= \sum_{i=1}^K \mathbf{1}\{k = k^*\} W_{i,k} (-X_{i,k}) + \sum_{k=1}^K W_{i,k} P_{i,k} X_{i,k}. \end{aligned}$$

Continuing, we have

$$\begin{aligned} \frac{\partial^2 \ell_1(V_i, \vec{C}_i, \vec{W}_i, C_i^*, Y_i)}{\partial \beta_0^2} &= \sum_{i=1}^K P_{i,k} X_{i,k} X_{i,k}^\top - \left(\sum_{k=1}^K P_{i,k} X_{i,k} \right) \left(\sum_{k=1}^K P_{i,k} X_{i,k} \right)^\top, \\ \frac{\partial^2 \ell_1(V_i, \vec{C}_i, \vec{W}_i, C_i^*, Y_i)}{\partial \beta_1^2} &= \sum_{i=1}^K P_{i,k} W_{i,k} X_{i,k} X_{i,k}^\top - \left(\sum_{k=1}^K W_{i,k} P_{i,k} X_{i,k} \right) \left(\sum_{k=1}^K W_{i,k} P_{i,k} X_{i,k} \right)^\top. \end{aligned}$$

Let d be the dimension of $X_{i,k}$. For any unit $x \in \mathbb{R}^d$, we have

$$\begin{aligned} x^\top \frac{\partial^2 \ell_1(V_i, \vec{C}_i, \vec{W}_i, C_i^*, Y_i)}{\partial \beta_0^2} x &= \sum_{k=1}^K P_{i,k} (X_{i,k}^\top x)^2 - \left(\sum_{k=1}^K P_{i,k} X_{i,k}^\top x \right)^2, \\ &= \sum_{k_1=1}^K P_{i,k_1} \sum_{k_2=1}^K P_{i,k_2} (X_{i,k_1}^\top x)^2 - \left(\sum_{k=1}^K P_{i,k} X_{i,k}^\top x \right)^2 \\ &= \sum_{k_1 < k_2}^K P_{i,k_1} P_{i,k_2} (X_{i,k_1}^\top x - X_{i,k_2}^\top x)^2. \end{aligned}$$

Denote x_{k_1, k_2} as a concatenated vector of K subvectors of length d , with its k_1 -th and k_2 -th sub-vectors being x . Denote $M(k_1, k_2, a_1, a_2)$ as a row-concatenated matrix of K submatrices of size $d \times d$, with its k_1 -th and k_2 -th sub-matrices being $a_1 I$ and $a_2 I$. Since $P_{i,k}$ is the exposure probability, and thus we have

$$\begin{aligned} x^\top \frac{\partial^2 \ell_1(V_i, \vec{C}_i, \vec{W}_i, C_i^*, Y_i)}{\partial \beta_0^2} x &\leq \sum_{k_1 < k_2}^K (X_{i,k_1}^\top x - X_{i,k_2}^\top x)^2 = x^\top \sum_{k_1 < k_2} (X_{i,k_1} - X_{i,k_2})(X_{i,k_1} - X_{i,k_2})^\top x \\ &= \sum_{k_1 < k_2} x_{k_1, k_2}^\top M(k_1, k_2, 1, -1)^\top \Sigma M(k_1, k_2, 1, -1) x_{k_1, k_2} \\ &\leq C \sum_{k_1 < k_2} x_{k_1, k_2}^\top M(k_1, k_2, 1, -1)^\top M(k_1, k_2, 1, -1) x_{k_1, k_2} \\ &= CK(K-1) \|x\|_2^2. \end{aligned}$$

Also under Assumption 2, we have $P_{i,k} \geq \delta$, and thus

$$\begin{aligned} x^\top \frac{\partial^2 \ell_1(V_i, \vec{C}_i, \vec{W}_i, C_i^*, Y_i)}{\partial \beta_0^2} x &\geq \delta^2 \sum_{k_1 < k_2}^K (X_{i,k_1}^\top x - X_{i,k_2}^\top x)^2 = x^\top \delta^2 \sum_{k_1 < k_2} (X_{i,k_1} - X_{i,k_2})(X_{i,k_1} - X_{i,k_2})^\top x \\ &= \delta^2 \sum_{k_1 < k_2} x_{k_1, k_2}^\top M(k_1, k_2, 1, -1)^\top \Sigma M(k_1, k_2, 1, -1) x_{k_1, k_2} \\ &\geq \delta^2 c \sum_{k_1 < k_2} x_{k_1, k_2}^\top M(k_1, k_2, 1, -1)^\top M(k_1, k_2, 1, -1) x_{k_1, k_2} \\ &= \delta^2 c K(K-1) \|x\|_2^2. \end{aligned}$$

Collectively, for $\mathcal{I}_0 = \mathbb{E}[\frac{\partial^2 \ell_1(V_i, \vec{C}_i, \vec{W}_i, C_i^*, Y_i)}{\partial \beta_0^2}]$, we have its eigenvalues bounded between $[K(K-1)c\delta^2, K(K-1)C]$.

Similarly,

$$\begin{aligned} x^\top \frac{\partial^2 \ell_1(V_i, \vec{C}_i, \vec{W}_i, C_i^*, Y_i)}{\partial \beta_1^2} x &= \sum_{k=1}^K P_{i,k} (W_{i,k} X_{i,k}^\top x)^2 - \left(\sum_{k=1}^K P_{i,k} W_{i,k} X_{i,k}^\top x \right)^2, \\ &= \sum_{k_1=1}^K P_{i,k_1} \sum_{k_2=1}^K P_{i,k_2} (W_{i,k} X_{i,k_1}^\top x)^2 - \left(\sum_{k=1}^K P_{i,k} W_{i,k} X_{i,k}^\top x \right)^2 \\ &= \sum_{k_1 < k_2}^K P_{i,k_1} P_{i,k_2} (W_{i,k_1} X_{i,k_1}^\top x - W_{i,k_2} X_{i,k_2}^\top x)^2. \end{aligned}$$

So we have

$$\begin{aligned} x^\top \frac{\partial^2 \ell_1(V_i, \vec{C}_i, \vec{W}_i, C_i^*, Y_i)}{\partial \beta_1^2} x &\leq x^\top \sum_{k_1 < k_2} (W_{i,k_1} X_{i,k_1} - W_{i,k_2} X_{i,k_2})(W_{i,k_1} X_{i,k_1} - W_{i,k_2} X_{i,k_2})^\top x \\ &= \sum_{k_1 < k_2} x_{k_1, k_2}^\top M(k_1, k_2, W_{i,k_1}, -W_{i,k_2})^\top \Sigma M(k_1, k_2, W_{i,k_1}, -W_{i,k_2}) x_{k_1, k_2} \leq \sum_{k_1 < k_2} C \|x\|_2^2 (W_{i,k_1} + W_{i,k_2}), \end{aligned}$$

so the eigenvalues of \mathcal{I}_1 are upper bounded by $\sum_{k_1 < k_2} 2qC = K(K-1)qC$. Also,

$$\begin{aligned} x^\top \frac{\partial^2 \ell_1(V_i, \vec{C}_i, \vec{W}_i, C_i^*, Y_i)}{\partial \beta_1^2} x &\geq \delta^2 x^\top \sum_{k_1 < k_2} (W_{i,k_1} X_{i,k_1} - W_{i,k_2} X_{i,k_2})(W_{i,k_1} X_{i,k_1} - W_{i,k_2} X_{i,k_2})^\top x \\ &= \delta^2 \sum_{k_1 < k_2} x_{k_1, k_2}^\top M(k_1, k_2, W_{i,k_1}, -W_{i,k_2})^\top \Sigma M(k_1, k_2, W_{i,k_1}, -W_{i,k_2}) x_{k_1, k_2} \\ &\geq c\delta^2 \sum_{k_1 < k_2} \|x\|_2^2 (W_{i,k_1} + W_{i,k_2}), \end{aligned}$$

so the eigenvalues of \mathcal{I}_1 are lower bounded by $\delta^2 \sum_{k_1 < k_2} 2qc = K(K-1)qc\delta^2$.

Appendix D: Limiting Theorems for Debiased Estimator

We prove the below theorem to show the asymptotic regularity of our debiased estimator.

THEOREM 1. *Suppose that Assumptions 1 & 2 hold. Assume that the data generating process follows the recommender choice model Equation (7) and the viewer response model Equation (8). Suppose that the nuisance estimates are all bounded by the constant C in Assumption 2 and satisfy the convergence rate: $\|\hat{s}_0 - s_0\|_{L_2} + \|\hat{s}_1 - s_1\|_{L_2} + \|\hat{z} - z\|_{L_2} = o(n^{-1/4})$ and $\|\hat{H} - H\|_{L_2} = o(n^{-1/4})$. Then, the double/debiased estimator $\hat{\tau}_n^{DB}$ in (18) is \sqrt{n} -consistent with $\hat{\tau}_n^{DB} - \tau = O_p(n^{-1/2})$.*

Define the estimated variance as:

$$\hat{V}_n = \frac{1}{n} \sum_{i=1}^n \left(\psi(V_i, \vec{C}_i, \vec{W}_i, k_i^*, Y_i; \hat{s}_0, \hat{s}_1, \hat{z}, \hat{H}) - \hat{\tau}_n^{DB} \right)^2. \quad (19)$$

If \hat{V}_n converges in probability to a constant, then $\hat{\tau}_n^{DB}$ is asymptotically normal with: $\sqrt{n}(\hat{\tau}_n^{DB} - \tau) / \sqrt{\hat{V}_n} \Rightarrow \mathcal{N}(0, 1)$.

Define

$$\tilde{\tau}_n^{DB} = \frac{1}{n} \sum_{i=1}^n \psi(V_i, \vec{C}_i, \vec{W}_i, k_i^*, Y_i; s_0, s_1, z, H), \quad (37)$$

with that

$$\begin{aligned} \psi(V_i, \vec{C}_i, \vec{W}_i, k_i^*, Y_i; s_0, s_1, z, H) &= \mu(V_i, \vec{C}_i; s_0, s_1, z) \\ &\quad - \nabla \mu(V_i, \vec{C}_i; s_0, s_1, z)^T H(V_i, \vec{C}_i; s_0, s_1, z)^{-1} \nabla \ell(V_i, \vec{C}_i, \vec{W}_i, k_i^*, Y_i; s_0, s_1, z). \end{aligned} \quad (38)$$

Note that

$$\mathbb{E}[\psi(V_i, \vec{C}_i, \vec{W}_i, k_i^*, Y_i; s_0, s_1, z, H) \mid V_i, \vec{C}_i] = \mu(V_i, \vec{C}_i; s_0, s_1, z), \quad (39)$$

by the first order condition of (s_0, s_1, z) in ℓ when conditioning on $(V_i, \vec{C}_i, \vec{W}_i)$. Our goal is to show that

- (i) $\hat{\tau}_n^{DB}$ and $\tilde{\tau}_n^{DB}$ have similar asymptotic behavior;
- (ii) asymptotic regularity of $\tilde{\tau}_n^{DB}$.
- (iii) asymptotically consistent variance estimator.

D.1. Step I: connecting $\hat{\tau}_n$ to $\tilde{\tau}_n$.

This part's proof is largely motivated by the proof pattern for Theorem 3.1 in [Chernozhukov et al. \(2018\)](#), though we need to additionally deal with the correlation among samples due to the shared items in their consideration sets. For notation convenience, define $\theta_0 = (s_0, s_1, z, H)$ and $\hat{\theta}_0 = (\hat{s}_0, \hat{s}_1, \hat{z}, \hat{H})$. Write $Z_i := (V_i, \vec{C}_i, \vec{W}_i, k_i^*, Y_i)$. Note that

$$\mathbb{E} \left[\psi(Z_i; \theta_0) \mid V_i, \vec{C}_i, \vec{W}_i \right] \stackrel{(i)}{=} \mathbb{E} \left[\mu \left(V_i, \vec{C}_i; s_0, s_1, z \right) \mid V_i, \vec{C}_i, \vec{W}_i \right] = \mu \left(V_i, \vec{C}_i; s_0, s_1, z \right), \quad (40)$$

where (i) is by the first-order optimality of (s_0, s_1, z) in ℓ . We have

$$\sqrt{n} \left| \hat{\tau}_n^{DB} - \tilde{\tau}_n^{DB} \right| \leq I_1 + I_2, \quad (41)$$

where

$$\begin{aligned} I_1 &:= \left\| \frac{1}{\sqrt{n}} \sum_i \left(\psi(Z_i; \hat{\theta}_0) - \mathbb{E}[\psi(Z_i; \hat{\theta}_0)] \right) - \frac{1}{\sqrt{n}} \sum_i \left(\psi(Z_i; \theta_0) - \mathbb{E}[\psi(Z_i; \theta_0)] \right) \right\|, \\ I_2 &:= \left\| \sqrt{n} \left(\mathbb{E}[\psi(Z_i; \hat{\theta}_0)] - \mathbb{E}[\psi(Z_i; \theta_0)] \right) \right\|. \end{aligned}$$

We now bound I_1 and I_2 respectively.

Bounding I_1 . Write $Q_i := \left(\psi(Z_i; \hat{\theta}_0) - \mathbb{E}[\psi(Z_i; \hat{\theta}_0)] \right) - \left(\psi(Z_i; \theta_0) - \mathbb{E}[\psi(Z_i; \theta_0)] \right)$. We have

$$\begin{aligned} \mathbb{E}[I_1^2] &= \frac{1}{n} \mathbb{E} \left[\left(\sum_i Q_i \right)^2 \right] = \frac{1}{n} \sum_i \mathbb{E}[Q_i^2] + \frac{1}{n} \sum_i \sum_{j \neq i} \mathbf{1}(\vec{W}_i \cap \vec{W}_j \neq \emptyset) \mathbb{E}[Q_i Q_j] \\ &= \frac{O(a_n)}{n} \sum_i \mathbb{E}[Q_i^2] = O\left(\frac{a_n}{n}\right) \sum_i \mathbb{E} \left[\left\{ \left(\psi(Z_i; \hat{\theta}_0) - \mathbb{E}[\psi(Z_i; \hat{\theta}_0)] \right) - \left(\psi(Z_i; \theta_0) - \mathbb{E}[\psi(Z_i; \theta_0)] \right) \right\}^2 \right] \end{aligned} \quad (42)$$

$$\leq O\left(\frac{a_n}{n}\right) \sum_i \mathbb{E} \left[\left(\psi(Z_i; \hat{\theta}_0) - \psi(Z_i; \theta_0) \right)^2 \right] = O(a_n \epsilon_n^2). \quad (43)$$

Therefore, by Markov inequality, we have $I_1 = O_p(a_n^{1/2} \epsilon_n)$.

Bounding I_2 . Define the function

$$f(r) := \mathbb{E}[\psi(Z_i; \theta_0 + r(\hat{\theta}_0 - \theta_0))] - \mathbb{E}[\psi(Z_i; \theta_0)], \quad r \in (0, 1). \quad (44)$$

By Taylor expansion, we have

$$f(1) = f(0) + f'(0) + f''(\tilde{r})/2, \quad \text{for some } \tilde{r} \in (0, 1). \quad (45)$$

Note that by the Neyman orthogonality (shown in [B.3](#)), we have $f'(0) = 0$. With the bounded inverse of Hessian, we have

$$\mathbb{E}[\|f''(\tilde{r})\|] \leq \sup_{r \in (0, 1)} \|f''(r)\| = O(\epsilon_n^2). \quad (46)$$

We have

$$I_{2,k} = O_p(\sqrt{n} \epsilon_n^2). \quad (47)$$

Combining the bound for I_1 and I_2 , we have

$$\sqrt{n} (\hat{\tau}_n^{DB} - \tilde{\tau}_n^{DB}) = O_p(a_n^{1/2} \epsilon_n + n^{1/2} \epsilon_n^2) = o_p(1), \quad (48)$$

with $a_n = O(n^{1/4})$ and $\epsilon_n = o(n^{-1/4})$.

D.2. Step II: characterizing the asymptotic behavior of $\tilde{\tau}_n$.

Recall the data generating process: when a new viewer V_i arrives, the back-end retrieval system firstly generates the consideration set \vec{C}_i . For content items that have shown in previous samples, the treatment status remains unchanged. For content items that haven't appear, we sample the treatment status from i.i.d. Bernoulli randomized trials. This procedure constructs the treatment collection \vec{W}_i . Then given $(V_i, \vec{C}_i, \vec{W}_i)$, the recommender chooses item k_i^* to expose, yielding the viewer outcome Y_i and the observation tuple $Z_i := (V_i, \vec{C}_i, \vec{W}_i, k_i^*, Y_i)$. We now apply the martingale theorem to analyze the asymptotic behavior of $\tilde{\tau}_n$. Denote the σ -field $\mathcal{F}_i := \sigma(Z_1, \dots, Z_i)$. We have that

$$\begin{aligned} \mathbb{E}[\psi(Z_i; \theta_0) | \mathcal{F}_{i-1}] &= \mathbb{E} \left[\mathbb{E} [\psi(Z_i; \theta_0) | V_i, \vec{C}_i, \vec{W}_i] | \mathcal{F}_{i-1} \right] \\ &= \mathbb{E} \left[\mathbb{E} [\mu(V_i, \vec{C}_i; \theta_0) | V_i, \vec{C}_i, \vec{W}_i] | \mathcal{F}_{i-1} \right] = \mathbb{E} [\mu(V_i, \vec{C}_i; \theta_0)] = \tau. \end{aligned}$$

Therefore $\{\psi(Z_i; \theta_0) - \tau\}$ forms a martingale difference sequence with respect to filtration $\{\mathcal{F}_i\}$. We now apply the following result from [Hall and Heyde \(2014\)](#).

PROPOSITION 3 (Martingale Central Limit Theorem, Theorem 3.2, [Hall and Heyde \(2014\)](#)).

Let $\{\xi_i\}$ be a martingale difference sequence with respect to filtration $\{\mathcal{F}_i\}$, and let η^2 be an a.s. finite random variable. Suppose that:

$$\max_i |\xi_i| \xrightarrow{p} 0, \quad (49)$$

$$\sum_i \xi_i^2 \xrightarrow{p} \eta^2, \quad (50)$$

$$\mathbb{E}[\max_i \xi_i^2] \text{ is bounded.} \quad (51)$$

Then $\sum_{i=1}^n X_i \xrightarrow{d} Z$ (stably), where the random variable Z has characteristic function $\mathbb{E}[\exp(-\frac{1}{2}\eta^2 t^2)]$.

Now let's verify the above conditions for $\sqrt{n}(\tilde{\tau} - \tau)$. Define

$$\xi_i = \frac{1}{\sqrt{n}} \{\psi(Z_i; \theta_0) - \tau\}.$$

We have $\mathbb{E}[\xi_i | \mathcal{F}_{i-1}] = 0$. By the bounded inverse of Hessian, we have $|\xi_i| = O(n^{-1/2})$, implying (49) and (51).

Also, we have

$$\sum_i \xi_i^2 = \frac{1}{n} \sum_i (\psi_i(Z_i; \theta_0) - \tau)^2 = O(1).$$

Let η^2 be the limiting random variable of $\sum_i \xi_i^2$, and thus η^2 is bounded a.s., verifying (50). We thus have

$$\sqrt{n}(\tilde{\tau}_n^{DB} - \tau) = \sum_i \xi_i \xrightarrow{d} z, \quad (52)$$

where z has characteristic function $\mathbb{E}[\exp(-\frac{1}{2}\eta^2 t^2)]$, implying a bounded variance of $\mathbb{E}[\eta^2]$. Connecting (52) with (48), by Slutsky's theorem, we have

$$\sqrt{n}(\hat{\tau}_n^{DB} - \tau) = \sqrt{n}(\hat{\tau}_n^{DB} - \tilde{\tau}_n^{DB}) + \sqrt{n}(\tilde{\tau}_n^{DB} - \tau) \xrightarrow{d} z, \quad (53)$$

yielding that $\hat{\tau}_n^{DB} - \tau = O_p(n^{-1/2})$.

D.3. Step III: connecting \tilde{V}_n to \hat{V}_n .

When \tilde{V}_n converges in the sense that

$$\tilde{V}_n := \frac{1}{n} \sum_i (\psi_i(Z_i; \theta_0) - \tau)^2 \xrightarrow{p} \eta^2,$$

with η^2 being a constant, then the characteristic function $\mathbb{E}[\exp(-\frac{1}{2}\eta^2 t^2)]$ is linked to a Gaussian distribution with variance η^2 , and $\sqrt{n}(\hat{\tau}_n^{DB} - \tau)$ converges in distribution to $\mathcal{N}(0, \eta^2)$.

Note that \tilde{V}_n by definition is a consistent η^2 estimator. We now show that \hat{V}_n is also a consistent variance estimator for η^2 . By the convergence of $\hat{\theta}_0$ to θ_0 and the boundedness of $\psi(Z_i; \hat{\theta}_0)$ and $\psi(Z_i; \theta_0)$, we have

$$\begin{aligned} |\hat{V}_n - \tilde{V}_n| &= \left| \frac{1}{n} \sum_i \left(\psi(Z_i; \hat{\theta}_0) - \psi(Z_i; \theta_0) \right) \left(\psi(Z_i; \hat{\theta}_0) + \psi(Z_i; \theta_0) \right) \right| \\ &\leq O(1) \cdot \frac{1}{n} \sum_i \left| \psi(Z_i; \hat{\theta}_0) - \psi(Z_i; \theta_0) \right| = O_p(\|\hat{\theta}_0 - \theta_0\|_{L_2}) = O_p(\epsilon_n) = o_p(1). \end{aligned}$$

In order to show \hat{V}_n is also a consistent variance estimator for η^2 , we only need to show that η^2 is a positive constant bounded away from 0 and ∞ , as demonstrated below.

From $\tilde{V}_n = O(1)$, we have $\eta^2 = O(1)$. For the lower bound of η^2 , consider

$$\tilde{V}_n = \frac{1}{n} \sum_i (\psi_i(Z_i; \theta_0) - \tau)^2 = \frac{1}{n} \sum_i (\mu(V_i, \vec{C}_i; \theta_0) - \tau - \phi_i)^2,$$

$$\text{where } \phi_i := \nabla \mu(V_i, \vec{C}_i; s_0, s_1, z)^T H(V_i, \vec{C}_i; s_0, s_1, z)^{-1} \nabla \ell(V_i, \vec{C}_i, \vec{W}_i, k_i^*, Y_i; s_0, s_1, z).$$

Then we have

$$\begin{aligned} \mathbb{E}[\tilde{V}_n] &= \frac{1}{n} \sum_i \mathbb{E}[(\mu(V_i, \vec{C}_i; \theta_0) - \tau - \phi_i)^2] \\ &= \frac{1}{n} \sum_i \mathbb{E}\left[\left\{\mu(V_i, \vec{C}_i; \theta_0) - \tau\right\}^2\right] - 2 \frac{1}{n} \sum_i \mathbb{E}\left[\left\{\mu(V_i, \vec{C}_i; \theta_0) - \tau\right\} \mathbb{E}[\phi_i | \mathcal{F}_{i-1}, V_i, \vec{C}_i, \vec{W}_i]\right] + \frac{1}{n} \sum_i \mathbb{E}[\phi_i^2] \\ &= \frac{1}{n} \sum_i \mathbb{E}\left[\left\{\mu(V_i, \vec{C}_i; \theta_0) - \tau\right\}^2\right] + \frac{1}{n} \sum_i \mathbb{E}[\phi_i^2], \end{aligned}$$

where the last inequality uses the first-order optimality of θ_0 in ℓ . Note that $\{\mu(V_i, \vec{C}_i; \theta_0)\}$ are i.i.d. random variable with mean τ , we thus have $\mathbb{E}[\tilde{V}_n] \geq \text{Var}(\mu(V_i, \vec{C}_i; \theta_0)) := \sigma^2$. Recall that \tilde{V}_n is also bounded, we have \tilde{V}_n converges to η^2 in expectation as well, which leads to

$$0 < \sigma^2 \leq \lim_{n \rightarrow \infty} \mathbb{E}[\tilde{V}_n] = \mathbb{E}\left[\lim_{n \rightarrow \infty} \tilde{V}_n\right] = \eta^2, \quad (54)$$

showing that η^2 is bounded away from 0 and ∞ , concluding our proof.

Appendix E: General Case of Multiple Treatments

Let L be the number of different treatments and n be the sample size of collected recommendations during the experiment. Each sample i provides an observation $(V_i, \vec{C}_i, \vec{W}_i, k_i^*, Y_i)$, we use $V_i \in \mathcal{V}$ to denote viewer embedding and $\vec{C}_i = \{C_{i,k} : C_{i,k} \in \mathcal{I}\}_{k=1}^K$ to denote the item embedding in the consideration set. We use $\vec{W}_i = \{W_{i,k}\}_{k=1}^K$ to denote the treatment set of candidate content items, each of which is randomized into either the control group with probability p_0 (where $W_{i,k} = 0$ and the status-quo algorithm is applied), or treatment group l with probability p_l (where $W_{i,k} = l$ and the l -th treatment is applied); note that $\sum_{l=0}^L p_l =$

1. Post-treatment, we use k_i^* to denote the index of recommended item and Y_i as the corresponding viewer response towards item k_i^* .

The key quantity ATE, for each treatment l , is defined as follows:

$$\tau_l := \mathbb{E}[Y_i | \vec{W}_i = \{l, \dots, l\}] - \mathbb{E}[Y_i | \vec{W}_i = \{0, \dots, 0\}], \quad (55)$$

We next describe our model under the multiple treatment settings, which illuminates how interference happens during the recommendation process, just like the binary treatment case outlined in the main body.

E.1. Recommender Choice Model

Given a viewer V_i , the goal of the recommender is to select the most relevant item from the consideration set \vec{C}_i to optimize her experience. As outlined in Section 2.1, industry-standard recommender systems usually consist of a long pipeline that involves multiple evaluation stages. We follow the concept of *model distillation* Hinton et al. (2015) and transfer the evaluation process – from the stage where treatment applies to the end stage where one content item is selected for exposure – into a summarized evaluation vector $\vec{S}_i = (S_{i,1}, \dots, S_{i,K})$, where in particular, the score $S_{i,k}$ of each content item $C_{i,k}$ takes the following semi-parametric form:

$$S_{i,k} = s_0(V_i, C_{i,k}) + \sum_{l=1}^L \mathbf{1}\{W_{i,k}=l\} \cdot s_l(V_i, C_{i,k}) + \epsilon_{i,k}. \quad (56)$$

Above, $s^0(\cdot, \cdot)$ generates the baseline score, which approximates recommender evaluation in the control status; and $s_l(\cdot, \cdot)$ generates score uplift (as compared to the control) when treatment l is applied (for example, s_l can be interpreted as the item boosting effect of cold-start algorithm l as compared to the status-quo). In particular, these score functions are heterogeneous across viewers and content items, laying foundations for personalized recommendations. The error term $\epsilon_{i,k}$ represents the part of evaluation that score functions fail to capture, and we assume it follows the independent extreme value distribution.

Given scores \vec{S}_i , the recommender selects the item that wins the evaluation:

$$k_i^* = \arg \max_k S_{i,k}. \quad (57)$$

Following the choice model literature, the probability of the recommender choosing content item k is following the multinomial logit manner Train (2009):

$$\mathbb{P}\left(k_i^* = k \mid V_i, \vec{C}_i, \vec{W}_i\right) = \frac{e^{s_0(V_i, C_{i,k}) + \sum_{l=1}^L \mathbf{1}\{W_{i,k}=l\} \cdot s_l(V_i, C_{i,k})}}{\sum_{k'=1}^K e^{s_0(V_i, C_{i,k'}) + \sum_{l=1}^L \mathbf{1}\{W_{i,k'}=l\} \cdot s_l(V_i, C_{i,k'})}}. \quad (58)$$

Eq.(7) explicitly models the interference – the choice probability of one item will be affected by the treated status of other content items in the same consideration set.

E.2. Viewer Response Model

The viewer response model stays the same as the binary treatment settings. For completeness, we list it here as well. We assume that, conditional on the selected item by the recommender, the viewer's response is independent of other content items in the consideration set. With this, the outcome of viewer V_i can be represented in the following non-parametric way

$$Y_i = z(V_i, C_{i,k_i^*}) + \zeta_i, \quad (59)$$

where $z(\cdot, \cdot)$ shows the expected viewer response that is heterogeneous across viewer-content pairs, ζ_i is i.i.d. noise, and C_{i,k_i^*} is the selected item by the recommender.

E.3. Estimating Average Treatment Effect

Let treatment $\Omega \in \{1, \dots, L\}$ be the focal treatment that one seeks to evaluate against the control. The average treatment effect τ_Ω can be similarly constructed as:

$$\tau_\Omega = \mathbb{E}_{(V_i, \vec{C}_i)} \left[\sum_{k=1}^K z(V_i, C_{i,k}) \cdot \left\{ \frac{e^{s_0(V_i, C_{i,k}) + s_\Omega(V_i, C_{i,k})}}{\sum_{k'=1}^K e^{s_0(V_i, C_{i,k'}) + s_\Omega(V_i, C_{i,k'})}} - \frac{e^{s_0(V_i, C_{i,k})}}{\sum_{k'=1}^K e^{s_0(V_i, C_{i,k'})}} \right\} \right].$$

Given estimated nuisances $(\hat{s}_0, \hat{s}_1, \dots, \hat{s}_L, \hat{z})$, we have the direct ATE estimate for treatment Ω as:

$$\mu(V_i, \vec{C}_i; \hat{s}_0, \hat{s}_1, \hat{s}_\Omega, \hat{z}) = \sum_{k=1}^K \hat{z}(V_i, C_{i,k}) \cdot \left\{ \frac{e^{\hat{s}_0(V_i, C_{i,k}) + \hat{s}_\Omega(V_i, C_{i,k})}}{\sum_{k'=1}^K e^{\hat{s}_0(V_i, C_{i,k'}) + \hat{s}_\Omega(V_i, C_{i,k'})}} - \frac{e^{\hat{s}_0(V_i, C_{i,k})}}{\sum_{k'=1}^K e^{\hat{s}_0(V_i, C_{i,k'})}} \right\}.$$

We can similarly debias nuisance estimate errors using the procedure outlined in Section 4.2, constructing a double/debiased estimate $\psi(V_i, \vec{C}_i; \hat{s}_0, \hat{s}_1, \dots, \hat{s}_L, \hat{z})$. The explicit form of ψ is omitted here for brevity, but its derivation largely resembles the binary-treatment case and incorporates gradients of the direct estimate μ , the loss function ℓ , and the loss function's Hessian with respect to the nuisances. Note that although μ only depends on nuisances $(\hat{s}_0, \hat{s}_1, \hat{s}_\Omega, \hat{z})$, the gradient and Hessian of the loss function require all nuisances $(\hat{s}_0, \hat{s}_1, \dots, \hat{s}_L, \hat{z})$.

Appendix F: Discussion on Model Mis-specification

Our semi-parametric estimator, τ_n^{DR} , differs from the fully non-parametric double/debiased estimators exemplified by the Augmented Inverse Propensity Weighting (AIPW) in the causal inference literature, where both the outcome model and the propensity score are non-parametrically defined [Imbens \(2004\)](#). In contrast, the estimation and inference guarantees provided by our estimator, τ_n^{DR} , is within our modeling framework, particularly emphasizing that the recommended content is determined by the choice model delineated in Eq. (7). The following discussion shall explore the implications of model misspecification.

In the semi-parametric framework detailed in Section 3 of our study, the viewer response model is treated as fully nonparametric, contrasting with the choice model, which adopts a semi-parametric multinomial logit (MNL) structure. This MNL model integrates a non-parametric component that captures the context of viewers and consideration sets, alongside a parametric component that specifies the role of treatment. As a result, when the specified MNL model fails, the asymptotic properties and results presented in Section 4.2 might no longer be applicable.

As discussed in Section 2, the recommendation process is stochastic in nature. Given that the softmax function is capable of approximating any categorical distribution [Cervera et al. \(2021\)](#), we introduce the notation $s^*(\cdot) = \{s_1^*(\cdot), \dots, s_K^*(\cdot)\}$ to denote the ground truth logits:

$$\mathbb{P}(k_i^* = k \mid V_i, \vec{C}_i, \vec{W}_i; s^*) = \frac{e^{s_k^*(V_i, \vec{C}_i, \vec{W}_i)}}{\sum_{k'=1}^K e^{s_{k'}^*(V_i, \vec{C}_i, \vec{W}_i)}}.$$

Notably, in our choice model (7), we specify the logits as the below form:

$$s_k^*(V_i, \vec{C}_i, \vec{W}_i) = s_0(V_i, C_{i,k}) + W_{i,k} \cdot s_1(V_1, C_{i,k}). \quad (60)$$

EXAMPLE 1 (MISSPECIFICATION). Consider a toy example for M viewers with consideration sets of size K . Our choice model in (60) requires an estimation of $2KM$ parameters for baseline score s_0 and treatment score uplift s_1 , while the logit s^* in full generality requires estimation of $2^K KM$ parameters.

When (60) mis-specifies the true logit s^* , our specified model (s_0, s_1) in (60) is a projection of s^* , essentially approximating the true underlying logits within our modeling framework:

$$(s_0, s_1) = \arg \min_{\tilde{s}_0, \tilde{s}_1} \mathbb{E} \left[\ell_1(V_i, \vec{C}_i, \vec{W}_i, k_i^*; \tilde{s}_0, \tilde{s}_1) \right].$$

where the expectation is taken with respect to $(V_i, \vec{C}_i, \vec{W}_i, k_i^*)$ generated based on creator-side randomization for \vec{W} and the true choice model s^* for k_i^* . And in these cases, the asymptotic variance of $\hat{\tau}_n^{DR}$ aligns with the semi-parametric efficiency bound for the choice model outlined in (7) (see more discussion on robustness of doubly robust estimator under model misspecification in Chernozhukov et al. (2019)).

We finally mark the flexibility of our framework. With prior knowledge on how treatment affects the recommendations, one can adopt a more flexible function form of the treatment vector \vec{W} , such as kernel approximation, to better approximate its role in the true logits s^* , moving beyond the additive linear form in $W_{i,k}$ as specified in (60). As long as the chosen score function maintains a parametric relationship with the treatment status, the methodology outlined in this paper can be directly applied to construct a debiased estimator and obtain the corresponding estimation and inference results.

Appendix G: Simulation Details

In the simulation, a set of m content items are generated randomly, with a binary indicator of whether the content is of good quality. Key components are generated as follows:

1. Utility for each viewer-content pair: the utility score is randomly selected from $Exponential(\theta)$, where $\theta \sim \mathcal{N}(0, 1)$.
2. Indicator of whether the content is good: the binary feature is generated from $Bernoulli(0.5)$ distribution.
3. Treatment effect: if the content is in the control group, the baseline score s_0 is the baseline utility score; if the content is in the treatment group, the score will be uplifted by an uplift factor δ only if the content is good.
4. Outcome: the outcome for each viewer-content pair is solely determined by the baseline utility plus a random normal noise with mean 0 and variance 1.

In the simulation study, at each Monte Carlo simulation, we randomize over the treatment matrices but fix other components. We calculate the ground-truth ATE, which measures the difference in outcome from where the counterfactual treatment matrices of all one's and all zero's. Linear regression is used for fitting both the score functions (s_0, s_1) and the outcome model, with the input being (i) the binary feature of whether the video is good; and (ii) the utility score. We set the training epoch at 400 and plot the training loss decay across all three folds in Figure 9.

To evaluate the goodness of fit of our learned choice model, we compare it against both the ground truth choice model and a baseline model that assigns an equal probability of exposure to each item. Note that this baseline represents the maximum likelihood estimation of the choice model when no covariate information is used. Figure 10a and Figure 10b illustrate the ROC curves and the NDCG losses for all three models, respectively, with larger areas under the curve and smaller NDCG values indicating better performance.

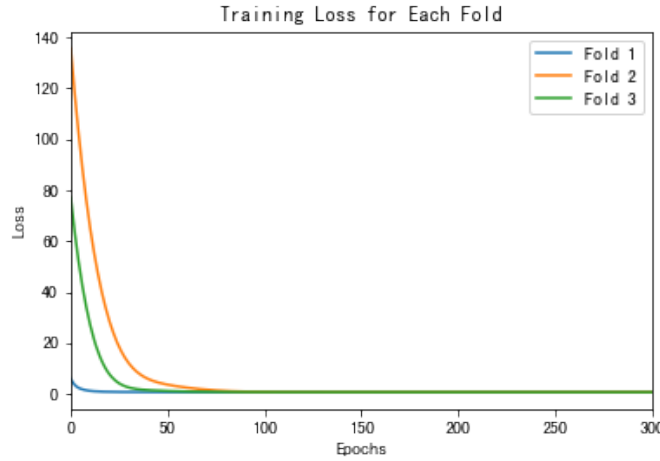
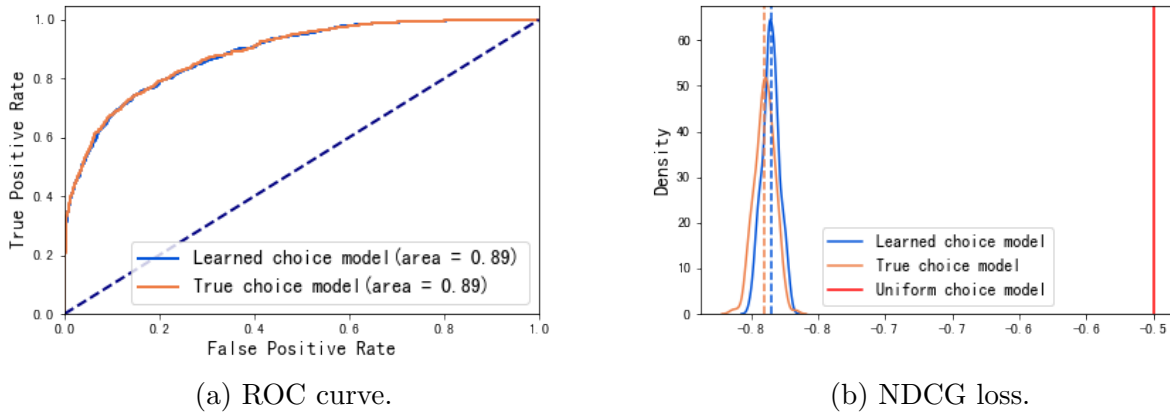


Figure 9 Training loss over the number of training epochs across different folds.



(a) ROC curve.

(b) NDCG loss.

Figure 10 Goodness of fit of learned choice model in simulations.

These results demonstrate that our learned choice model outperforms the baseline and closely approximates the ground truth choice model.

We also conduct a likelihood ratio test to compare our learned model against the null hypothesis represented by the baseline model. The network processes all inputs through an initial dense layer with a linear activation function, which comprises 3 parameters (2 for the features and 1 for the bias). Subsequently, each treatment is connected to a separate dense layer, also with 3 parameters. It is important to note that the baseline logit score for the first item in the consideration set is subtracted to ensure identifiability, resulting in a reduction of one degree of freedom. The baseline model, which represents the maximum likelihood estimation of the exposure probability for each video in the consideration set, thus has 4 degrees of freedom (5 parameters minus 1 for identification). We calculate the test statistic to be 2130, implying a p-value close to zero.